

**CEBAF**

The Continuous Electron Beam Accelerator Facility  
Theory Group Preprint Series

Additional copies are available from the authors.

The Southeastern Universities Research Association (SURA) operates the Continuous Electron Beam Accelerator Facility for the United States Department of Energy under contract DE-AC05-84ER40150

**DISCLAIMER**

This report was prepared as an account of work sponsored by the United States government. Neither the United States nor the United States Department of Energy, nor any of their employees, makes any warranty, express or implied, or assumes any legal liability or responsibility for the accuracy, completeness, or usefulness of any information, apparatus, product, or process disclosed, or represents that its use would not infringe privately owned rights. Reference herein to any specific commercial product, process, or service by trade name, mark, manufacturer, or otherwise, does not necessarily constitute or imply its endorsement, recommendation, or favoring by the United States government or any agency thereof. The views and opinions of authors expressed herein do not necessarily state or reflect those of the United States government or any agency thereof.

**Electromagnetic Properties of the Pion as a Composite Nambu-Goldstone Boson**

Hiroshi Ito<sup>†</sup>, W. W. Buck

Department of Physics, Hampton University  
Hampton, Virginia 23668, U.S.A.

Franz Gross

Physics Department, College of William and Mary  
Williamsburg, Va. 23185, U.S.A.

and

Continuous Electron Beam Accelerator Facility  
12000 Jefferson Avenue, Newport News, Va. 23606

**Abstract**

Motivated by the Nambu-Jona-Lasinio model of light mesons, we introduce a covariant separable interaction to model the structure of relativistic quark-antiquark systems. The Schwinger-Dyson equation for the quark self-energy is solved analytically, generating a dynamical quark mass through spontaneous breaking of chiral symmetry, and yielding a pion which has zero mass in the chiral limit. The Bethe-Salpeter vertex function for this  $q\bar{q}$ -pion, which has a momentum distribution and composite structure associated with the interaction, is obtained analytically. Using this vertex function, and a similar one for the  $\rho$  meson, we calculate the electromagnetic observables of this composite Nambu-Goldstone boson, including effects from  $\rho$ -meson dominance processes. Our calculation takes the composite structure of the mesons into account. The  $\rho$  meson effects are found to be very small in the pion charge form factor, but substantial in the charge radius. Using the model, predictions are made for  $\gamma^*\pi^0 \rightarrow \gamma$  and  $\rho\pi\gamma$  transition form factors.

## I. Introduction

It is well known that the pion plays an important role in the description of nuclear dynamics. Its lightness as a Nambu-Goldstone (NG) boson<sup>1,7</sup> means that it dominates the long-range and low-energy aspects of nuclear dynamics. The low-energy theorems<sup>2</sup> obtained with the PCAC hypothesis and current algebra<sup>3</sup> for point-like objects work extremely well in the low energy region of nuclear dynamics<sup>4</sup>, including electromagnetic reactions<sup>5</sup>. As the energy scale is increased, however, the intrinsic structure of the pion should be taken into account, and various electromagnetic observables depend on this structure. In this paper, we explore the electromagnetic properties of the pion as a NG boson with a composite structure.

In this respect it would be very meaningful to develop a model in which both the spontaneous breaking of chiral symmetry<sup>6</sup> is realized, and a NG boson with a composite structure is obtained. The Nambu-Jona-Lasinio (NJL) model<sup>7</sup> is an example of a model satisfying the first requirement, and extensive investigations have been made using it<sup>8</sup>. The standard approach in the NJL model is to introduce a non-covariant momentum cutoff in order to assure that various loop integrals are finite. This approach does not provide a clear connection between the momentum distribution of the pion wave function and physical observables. It is more natural, useful, and realistic to introduce a momentum scale into the  $q\bar{q}$  interaction which will control the loop integrals; this can be done covariantly using a separable interaction. Combining this second requirement (finite momentum scale) with the NJL model is one of the objects of this paper. Such a procedure gives a clear connection between composite structure and physical observables.

In this paper we employ a chirally invariant, covariant, separable interaction model to describe the  $q\bar{q}$  interaction. Separable interactions are frequently used to treat pairing<sup>9</sup> in the BCS theory<sup>10</sup>, and here we take advantage of the simplicity with which the dynamical equations can be solved using a separable form. In our approach, the momentum scale of dynamical symmetry breaking can be associated with a range parameter ( $\Lambda$ ) appearing in the form factor of the separable interaction. Solving the Bethe-Salpeter equation is trivial with separable interactions, and we can associate the size of a composite pion

and the dynamically generated quark mass with this range parameter ( $\Lambda$ ). Compared to the standard use of the NJL model, our model relates the scale parameter  $\Lambda$  directly to the momentum distribution of the wave function, which is precisely defined by  $\Lambda$ . A consistent calculation of many observables including large momentum transfer processes is straightforward, still keeping the essence of the original NJL model.

Using the Hartree approximation at the one loop level, our model gives an analytic solution of the Schwinger-Dyson equation<sup>11,12</sup> for the quark self-energy  $\Sigma(q^2)$ , which goes like  $\sim \frac{1}{q^2}$  at large momentum. Thus the dynamical mass generated by spontaneous symmetry breaking has a momentum dependence which insures that it vanishes at large- $q^2$ . This behavior satisfies Polizer's criterion<sup>13</sup>, and therefore, in principle, our model can be applied to the calculations of observables in the asymptotic region, where quarks are almost massless and perturbative QCD is very successful.<sup>14</sup>

With the pion wave function obtained from the Bethe-Salpeter equation we calculate the physical observables associated with the pion. The charge form factor ( $F(q^2)$ ), charge radius ( $r_\pi$ ), weak decay constant ( $f_\pi$ ), two photon decay width ( $\Gamma_{\pi^0 \rightarrow \gamma\gamma}$ ) as well as  $\gamma^* \pi^0 \rightarrow \gamma$  transition form factor ( $F_{\gamma\pi}(q^2)$ ) are calculated. Here, we have only two model parameters; a constituent quark mass ( $m_q$ ) and a range parameter ( $\Lambda$ ) appearing in the rank-1 separable interaction. The results of our calculation are remarkably good in comparison with the experimental data, and the numerical values are very stable against variations of the parameters.

In electromagnetic processes, for example in the pion charge form factor, we have to take into account some important effects in addition to the standard impulse process (Fig.1). One effect is a contribution from the relativistic two-body current operator<sup>15</sup> due to interaction currents (Fig.2). This interaction current can transfer large momentum from the quark struck by the photon to the spectator quark. The interaction current is associated with the two-body interaction, and a consistent treatment is required both for the evaluation of wave functions and for the calculation of the matrix elements. The details of how to derive this relativistic two-body current operator have already been published<sup>16</sup>; the Ward-Takahashi identity and electromagnetic gauge invariance are used to constrain the current operator. We include this contribution in the charge form factor of

the pion by calculating the matrix elements of this relativistic two-body current operator; the derivation of the current operator itself will not be repeated here.

A second effect that occurs in the electromagnetic interaction is that of virtual vector mesons, which couple a photon to a hadron. Since the pion (as well as a vector meson) is a composite object, care must be taken in extending the usual Vector-Meson-Dominance (VMD) model<sup>17</sup> to space-like photon momentum<sup>18</sup>. For example, in the pion charge form factor, both the momentum dependence of the  $\rho\pi\pi$  triangle diagram and of the  $\rho\gamma$  coupling should be taken into account when the  $\rho$  is far off-mass shell, which is always the case for the space-like region. Furthermore, in the space-like region the propagator of a virtual  $\rho$  meson may not be the same as it is near the  $\rho$  pole. These effects are not included in the usual hadronic description of the VMD model, where the structure of the  $\rho$  meson is ignored.

Thus, a dynamical study will help to estimate not only the size, but momentum transfer region over which such vector meson processes are significant. Here again, a simple and explicit calculation is possible with a relativistic separable interaction. We extend the separable model of  $q\bar{q}$  interactions to the vector channel. The Bethe-Salpeter equation for the scattering matrix is solved analytically with the separable interaction, and the resulting scattering matrix is introduced into the *photon*  $\rightarrow$  *quark-antiquark* vertex (Fig.3). From the view of quark-meson duality<sup>19</sup>, the impulse  $\pi\pi\gamma$ -triangle diagram (Fig.1) may implicitly include the effect of a vector meson channel, but here we examine the additional correction explicitly without introducing double counting. Our result shows a very small contribution. In this paper we discuss electromagnetic gauge invariance of the photon propagator including this hadronic radiative correction.

This paper is organized in the following way. In Sec.II, the Bethe-Salpeter formalism with a relativistic separable interaction is reviewed, the Schwinger-Dyson equation for the quark self-energy is formulated and solved, the presence of a zero mass pion is demonstrated in the chiral limit, and the pion weak decay constant ( $f_\pi$ ), charge radius ( $r_\pi$ ), two-photon decay width ( $\Gamma_{\pi^0 \rightarrow \gamma\gamma}$ ), and the charge form factors are calculated. The effect of the interaction current is discussed in Sec. III. In Sec. IV, a covariant quark model of the  $\rho$ -meson is introduced, and the numerical effect of the vector meson process on the pion

charge form factor is presented as a correction to the impulse form factor. We predict the form factors of  $\gamma^*\pi^0 \rightarrow \gamma$  and  $\rho\pi\gamma$  processes in Sec. V, and summarize our work.

## II. Separable Interaction and Bethe-Salpeter equation

### A. Bethe-Salpeter equation

One of the most important aspects of the QCD lagrangian is that it is chirally symmetric in the light quark sector. The explicit symmetry breaking is very small due to the lightness of the u- and d-current quark mass ( $m_u + m_d \simeq 12MeV^{20}$ ); however dynamical breaking of chiral symmetry appears at the low energy scale to yield a constituent quark mass of  $m_q = 200 \sim 300MeV$ , and several dynamical models<sup>7,8,21,22</sup> address this issue. Here, we introduce a relativistic separable interaction with a chirally symmetric form, and the nature of the dynamical symmetry breaking is studied. As a consequence, the pion as a Nambu-Goldstone boson acquires a composite structure with a quark-antiquark ( $q\bar{q}$ ) momentum distribution associated with the interaction, and within this framework we calculate the electromagnetic observables.

We start with a general expression of the chiral invariant action ( $S_{\chi_2}$ ) for a four quark vertex,

$$S_{\chi_2} = \int \int \int \int d^4x_1 d^4x_2 d^4x'_1 d^4x'_2 K(x'_1, x'_2; x_1, x_2) \times \left[ (\bar{\Psi}(x'_1)I\Psi(x_1))(\bar{\Psi}(x'_2)I\Psi(x_2)) - (\bar{\Psi}(x'_1)\gamma^5\Psi(x_1))(\bar{\Psi}(x'_2)\gamma^5\Psi(x_2)) \right]. \quad (2.1)$$

Here,  $\tau$  is the Pauli matrix for the flavor space, and  $I$  is meant to be a diagonal matrix. This action is invariant under the global axial transformation  $\Psi(x) \rightarrow e^{i\gamma^5\tau\cdot\theta}\Psi(x)$  and  $\bar{\Psi}(x) \rightarrow \bar{\Psi}(x)e^{i\gamma^5\tau\cdot\theta}$ , independently of the structure of the kernel<sup>23</sup>  $K(x'_1, x'_2; x_1, x_2)$ . The kernel in the original Nambu-Jona-Lasinio model is a constant, and a momentum cut-off is introduced at  $\Lambda_{NJL} = 0.8 \sim 1GeV$  in the diverging loop integrals caused by the contact interaction. Other choices of the kernel will be found elsewhere<sup>24</sup>.

In our model, the generalized NJL interaction assumes a separable form

$$K(x'_1, x'_2 : x_1, x_2) = \frac{g}{2} f(|x'_1 - x_1|^2) f(|x'_2 - x_2|^2) I_{cs}, \quad (2.2)$$

where  $I_{cs} = \chi_c \otimes \chi_c^\dagger = \frac{1}{\sqrt{n_c}} I_{c'_1, c_1} \frac{1}{\sqrt{n_c}} I_{c'_2, c_2}$  is the projection operator for color singlet states, where  $c'_n$  and  $c_n$  are color indices. The number of colors is  $n_c$ . For flavor singlet states it may be possible to obtain this separable form from a multiple-gluon annihilation processes in the  $q\bar{q}$  channel,<sup>23</sup> but here we extend this idea to non-flavor singlet channels, and simply regard it as an empirical description of the interaction. In momentum space the separable interaction becomes

$$V_{\alpha\beta, \delta\gamma}(k', k) = g f(k'^2) f(k^2) \left[ I_{\alpha\beta} I_{\delta\gamma} - (\gamma^5 \tau)_{\alpha\beta} (\gamma^5 \tau)_{\delta\gamma} \right] I_{cs}, \quad (2.3)$$

where the Greek letters are used for the Lorenz and flavor indices (Fig. 4). Here,  $k' = (k'_1 + k'_2)/2$  is the relative momentum of the  $q\bar{q}$  pair in the final state, with a similar relation holding between unprimed variables for the initial state. We use a monopole form factor,  $f(k^2) = \frac{\Lambda^2}{k^2 + \Lambda^2}$ , with a parameter  $\Lambda$ , so that we can perform loop integrals by the standard Feynman parameter method. The Bethe-Salpeter equation for a bound state vertex (Fig.5) is given by

$$\Gamma_{\alpha\beta}(k'; p) = i \int \frac{d^4 k}{(2\pi)^4} V_{\alpha\beta, \delta\gamma}(k', k) S_{\gamma\alpha}(k + \frac{p}{2}) \Gamma_{\alpha\delta}(k; p) S_{\delta\beta}(k - \frac{p}{2}). \quad (2.4)$$

For a pseudoscalar-isovector state, the solution (defined at  $p^2 = m_b^2$ , where  $m_b$  is the mass of the bound state) has the form  $\Gamma(k; p) = \mathcal{N} \gamma^5 \mathcal{F}(k^2) \chi_c \chi_f$  with the wave function normalization  $\mathcal{N}$  to be determined by the charge normalization. Normalized wave functions for the color singlet and isovector flavor states are denoted respectively by  $\chi_c = \frac{1}{\sqrt{n_c}} I_{c', c}$  and  $\chi_f$  [ for example  $\chi_f = \frac{1}{\sqrt{2}} \tau_{f', f}$  for a neutral pion, where  $f$  is the flavor index ]. The quark propagator is defined by  $S(p) = [\not{p} - m_0 - \Sigma(p^2) + i\epsilon]^{-1}$  with the current quark mass

$m_0$ , and the quark self-energy  $\Sigma(p^2)$  given by a self-consistent equation. The equation for the  $q\bar{q}$  momentum distribution  $\mathcal{F}(k^2)$  becomes,

$$\mathcal{F}(k'^2) = -n_f g i \int \frac{d^4 k}{(2\pi)^4} \text{Tr} \left\{ \gamma^5 S(k + \frac{p}{2}) \gamma^5 S(k - \frac{p}{2}) \right\} f(k^2) \mathcal{F}(k^2). \quad (2.5)$$

The solution is  $\mathcal{F}(k^2) = f(k^2) \times \text{constant}$ , and we have the eigenvalue equation

$$1 = -n_f g i \int \frac{d^4 k}{(2\pi)^4} \text{Tr} \left\{ \gamma^5 S(k + \frac{p}{2}) \gamma^5 S(k - \frac{p}{2}) \right\} f^2(k^2). \quad (2.6)$$

For the zero mass pion ( $p^2 = 0$ ), eq (2.5) becomes

$$\mathcal{F}(k'^2) = 4n_f g i f(k'^2) \int \frac{d^4 k}{(2\pi)^4} f(k^2) \frac{\mathcal{F}(k^2)}{k^2 - [m_0 + \Sigma(k^2)]^2}, \quad (2.7)$$

where we used

$$\text{Tr} \left\{ \gamma^5 S(k + \frac{p}{2}) \gamma^5 S(k - \frac{p}{2}) \right\}_{p^2=0} = -4 [k^2 - (m_0 + \Sigma(k^2))]^{-1}.$$

## B. The Schwinger-Dyson equation

The self-consistent equation for the quark self energy (Fig.6a) is

$$\begin{aligned} \Sigma(k'^2) &= i \int \frac{d^4 k}{(2\pi)^4} V_{\alpha\beta, \delta\gamma}(k', k) S_{\gamma\delta}(k), \\ &= 4n_f g i f(k'^2) \int \frac{d^4 k}{(2\pi)^4} f(k^2) \frac{m_0 + \Sigma(k^2)}{k^2 - [m_0 + \Sigma(k^2)]^2}. \end{aligned} \quad (2.8)$$

The solution has a form  $\Sigma(k^2) = \text{constant} \times f(k^2)$ , and we write

$$\Sigma(k^2) = \kappa \Lambda^2 f(k^2) = \kappa \frac{\Lambda^2}{k^2 - \Lambda^2}. \quad (2.9)$$

In the chiral limit ( $m_0 = 0$ ), the equations for the  $q\bar{q}$  momentum distribution, eq (2.7), and for the quark self-energy, eq (2.8), become identical: if we have a nontrivial solution ( $\kappa \neq 0$ ), then a zero mass pion emerges as a Nambu-Goldstone boson with a momentum distribution given by  $\mathcal{F}(k^2)$ . A similar approach has been used to describe the instanton induced  $q\bar{q}$  interaction<sup>25</sup>, and the monopole form of the quark self energy was introduced by Cornwall.<sup>6</sup>

Inserting eq (2.9) into eq (2.8) with  $m_0 = 0$ , gives an equation for  $\kappa$

$$1 = 4in_f g \int \frac{d^4 k}{(2\pi)^4} f^2(k^2) \frac{1}{k^2 - \Sigma^2(k^2)} \\ = \frac{n_f g}{4\pi^2 \Lambda^2} \int_0^\infty dx \frac{x}{x(x+1)^2 + (\kappa/\Lambda)^2}. \quad (2.10)$$

Thus, the exact solution for the quark self-energy is given by eq (2.9) with  $\kappa$  determined by eq (2.10) for given values of  $g$  and  $\Lambda$ . Note that for  $g > g_c$  with  $g_c = \frac{4}{n_f} \pi^2 \Lambda^2$ , there exists a nontrivial solution,  $\kappa \neq 0$ .

In this paper we consider only the Hartree term (Fig.6a) in the Schwinger-Dyson equation. The Fock term (Fig.6b), which is of order  $\mathcal{O}(\frac{1}{n_c})$ , is neglected. This is the same approximation scheme used in the original NJL model. To be consistent, the exchange term is also not included in the eq (2.4). Nevertheless, if the Fock and exchange terms were included in eq (2.8) and eq (2.4), it can be shown that a zero mass pion still appears in the chiral limit. The explicit calculation of the quark self-energy including the Fock term is possible by following the method of Ref.27, but here we will not pursue this further.

### C. Observables

In the following calculation of physical observables, we approximate the momentum dependent quark self-energy by an effective mass  $m_q$ , so that  $k^2 - [m_0 + \Sigma(k^2)]^2 \rightarrow k^2 - m_q^2$ . Expanding around  $k^2 = m_q^2$ ,

$$k^2 - [m_0 + \Sigma(k^2)]^2 = Z(k^2 - m_q^2) + \mathcal{O}(|k^2 - m_q^2|^2), \quad (2.11)$$

8

gives an effective propagator of the form  $\frac{1}{Z(i\epsilon - m_q^2)}$  near the quark pole, and the constant  $Z$  can be removed by renormalizing the interaction strength. The low energy observables will be calculated using this effective propagator.

We now evaluate the pion weak decay constant ( $f_\pi$ ), two-photon decay width ( $\Gamma_{\pi^0 \rightarrow \gamma\gamma}$ ) and impulse charge form factor ( $F_{imp}(q^2)$ ) by using the pion vertex function

$$\Gamma(k; p) = \mathcal{N} \gamma^5 \mathcal{F}(k^2) \lambda_c \lambda_f.$$

Here the cutoff mass ( $\Lambda$ ) and the effective quark mass ( $m_q$ ) are the independent parameters fitted to the physical observables. The weak decay constant ( $f_\pi$ ) is given by calculating the diagram shown in Fig.7,

$$f_{\pi p^\mu} = \frac{\sqrt{n_c}}{i\sqrt{2}} \mathcal{N} \int \frac{d^4 k}{(2\pi)^4} \mathcal{F}(k^2) \text{Tr} \left\{ \gamma^5 \gamma^\mu S(k + \frac{p}{2}) \gamma^5 S(k - \frac{p}{2}) \right\}, \quad (2.12)$$

and the pion charge form factor in the impulse approximation is given by the impulse diagrams (Fig.1 and the other diagram where the photon couples to the  $\bar{d}$ -quark),

$$F_{imp}(q^2)(p' + p)^\mu = |\mathcal{N}|^2 \int \frac{d^4 k}{(2\pi)^4} \mathcal{F}^2(k^2) \text{Tr} \left\{ S(k - \frac{p}{2}) \gamma^5 S(k + \frac{p}{2} - q) \gamma^\mu S(k + \frac{p}{2}) \gamma^5 \right\}, \quad (2.13)$$

where the normalization ( $\mathcal{N}$ ) of wave function is determined by the charge normalization,  $F_{imp}(0) = 1$ . Note that the loop integrals for the charge form factor depend on  $\mathcal{F}^2(k^2)$ , while the one for the weak decay constant is linear in  $\mathcal{F}(k^2)$ . We emphasize that, in our generalization of the NJL model, the momentum cut-off is associated with the quark momentum distribution of the pion, and this effect therefore depends on the number of pion vertices in a given diagram. This is an essential difference from the original NJL model. The  $\pi\gamma\gamma$ -amplitude is calculated from the triangular diagrams (Fig.8) for the axial anomaly<sup>28,29,30</sup>,

$$M_{\pi\gamma\gamma} = t(k_1, \epsilon_1; k_2, \epsilon_2) + t(1 \leftrightarrow 2), \quad (2.14)$$

9

where

$$\begin{aligned} \langle (k_1, \epsilon_1; k_2, \epsilon_2) \rangle &= -iN \text{Tr} \{ Q_q Q_q \chi_f \} \sqrt{n_c} \\ &\times \int \frac{d^4 k}{(2\pi)^4} \mathcal{F}(k^2) \text{Tr} \left\{ f_2 S(k - \frac{k_1 - k_2}{2}) f_1 S(k + \frac{p}{2}) \gamma^5 S(k - \frac{p}{2}) \right\}. \end{aligned} \quad (2.15)$$

Here  $Q_q$  is the quark charge operator  $Q_q = \frac{1}{6}(1 + 3\tau^3)$ , and  $\chi_f = \frac{1}{\sqrt{2}}\tau^2$ . This amplitude can be expressed in a gauge invariant form

$$M_{\pi^0 \rightarrow \gamma\gamma} = A \epsilon_{\mu\nu\rho\sigma} \epsilon_1^\mu \epsilon_2^\nu k_1^\rho k_2^\sigma, \quad (2.16)$$

where

$$\begin{aligned} A &= 8m_q \mathcal{N} \sqrt{n_c} \text{Tr} \{ Q_q Q_q \chi_f \} \\ &\times (-i) \int \frac{d^4 k}{(2\pi)^4} \frac{\mathcal{F}(k^2)}{\left( \left[ k + \frac{k_1 - k_2}{2} \right]^2 - m_q^2 \right) \left( \left[ k + \frac{p}{2} \right]^2 - m_q^2 \right) \left( \left[ k - \frac{p}{2} \right]^2 - m_q^2 \right)} \end{aligned}$$

and the two-photon decay width is given by  $\Gamma_{\pi^0 \rightarrow \gamma\gamma} = \frac{m_\pi^2}{64\pi} \mathcal{A}^2$ .

The numerical results for these observables are plotted in Fig. 9 with several choices of  $\Lambda$  and  $m_q$ . Note that for a given quark mass, for example  $m_q = 250 \text{ MeV}$ , the two photon decay width is very stable under the variation of the cutoff mass  $\Lambda = 300$  to  $600 \text{ MeV}$ , and a very small deviation is found for the weak decay constant,  $f_\pi = 80$  to  $105 \text{ MeV}$ ; about 10% deviation from the experimental value of  $93 \text{ MeV}$ . For a fixed cutoff mass, for example  $\Lambda = 500 \text{ MeV}$ , the variations of these observables are also in the acceptable range for the quark mass,  $m_q = 230$  to  $280 \text{ MeV}$ . In addition, the charge radius has a slow dependence on the values of the cutoff mass and quark mass. The best fit is given by  $\Lambda = 450 \text{ MeV}$  and  $m_q = 248 \text{ MeV}$ , which gives  $f_\pi = 93 \text{ MeV}$  (93.),  $\Gamma_{\pi^0 \rightarrow \gamma\gamma} = 7.74 \text{ eV}$  ( $7.57 \pm 0.3^{31}$ ) and the charge radius  $r_\pi = 0.74(0.663 \pm 0.023^{32}) \text{ fm}$ , where the numbers in the parenthesis are the experimental values.

Inserting these best values ( $\Lambda = 450 \text{ MeV}$  and  $m_q = 248 \text{ MeV}$ ) into the Bethe-Salpeter eigenvalue eq. (2.6),

$$1 = -n_f g_i \int \frac{d^4 k}{(2\pi)^4} f^2(k^2) \frac{4m_q^2 + p^2 - 4k^2}{\left[ \left( k + \frac{p}{2} \right)^2 - m_q^2 \right] \left[ \left( k - \frac{p}{2} \right)^2 - m_q^2 \right]}, \quad (2.17)$$

gives  $g_0 = 2.795\pi^2 \Lambda^2$  if  $m_\pi = 140 \text{ MeV}$ . If we use this coupling constant in the zero mass eigenvalue equation,

$$1 = 4i n_f g_0 \int \frac{d^4 k}{(2\pi)^4} f^2(k^2) \frac{1}{[k^2 - M^2]}, \quad (2.18)$$

we get an effective quark mass of  $M = 234 \text{ MeV}$ , and a reasonable estimate for the current quark mass  $m_0 = 248 - 234 = 14 \text{ MeV}$ .

We predict the pion charge form factor by using the parameters obtained here. The numerical result for the impulse form factor (Fig.1) is presented in the next section along with the one for the two-body current contribution (Fig.2).

### III. Two-Body Interaction Currents.

When a large momentum is transferred to a many-body system, the momentum can be shared by each constituent through the two (or many)-body interaction. This two-body process, the interaction current, is an important correction to the impulse one-body process. The nonrelativistic treatment of this effect has an old history, but the relativistic treatment has been started only recently<sup>15,33</sup>.

The form of a relativistic two-body current must satisfy a general constraint, which is derived from current conservation and the Ward-Takahashi identity for the one-body current. By using minimal substitution methods<sup>34</sup> for introducing the gauge field into a nonlocal vertex, Ref.16 gives an explicit derivation of the two-body current operator for relativistic separable interactions. The result is expressed in terms of the two-body interaction and satisfies the general restriction. Here, we calculate the matrix elements of this current operator by using the bound state solution of the Bethe-Salpeter equation.

### A. Current Conservation and Interaction Currents.

If an external photon field couples to the bound state of the  $q\bar{q}$  system described by eq (2.4), the matrix element of the one-body impulse current is

$$\langle J_u^\mu \rangle = -i e_u \int \frac{d^4 k}{(2\pi)^4} \text{Tr} \left\{ \bar{\Psi}_f(k'; p') \gamma^\mu \Psi_i(k; p) S^{-1}(k - \frac{p}{2}) \right\} \quad (3.1a)$$

see Fig.1, and

$$\langle J_d^\mu \rangle = -i e_d \int \frac{d^4 k}{(2\pi)^4} \text{Tr} \left\{ \bar{\Psi}_f(k''; p') S^{-1}(k + \frac{p}{2}) \Psi_i(k; p) \gamma^\mu \right\}, \quad (3.1b)$$

where the Bethe-Salpeter wave function is related to the vertex function by  $\Psi(k; p) = S(k + \frac{p}{2}) \Gamma(k; p) S(k - \frac{p}{2})$ , and  $f$  and  $i$  denote the final and initial bound states (which need not be the same). The momentum variables are  $k' = k + \frac{p}{2}$  and  $k'' = k - \frac{p}{2}$ , and  $e_{u(d)}$  is the charge of the  $u(d)$ -quark. The impulse form factor is  $F_{i,mp}(q^2)[p+p']^\mu = \langle J_u^\mu \rangle + \langle J_d^\mu \rangle$ .

By using the Ward-Takahashi identity

$$\not{d} = S^{-1}(k + \frac{p}{2} + q) - S^{-1}(k + \frac{p}{2}), \quad (3.2)$$

the divergence of one-body current can be expressed as

$$\begin{aligned} q_\mu \langle J_u^\mu \rangle &= -i e_u \int \frac{d^4 k}{(2\pi)^4} \text{Tr} \left\{ S^{-1}(k - \frac{p}{2}) \bar{\Psi}_f(k + \frac{q}{2}; p') S^{-1}(k + \frac{p}{2} + q) \Psi_i(k; p) \right\} \\ &\quad + i e_u \int \frac{d^4 k}{(2\pi)^4} \text{Tr} \left\{ \bar{\Psi}_f(k + \frac{q}{2}; p') S^{-1}(k + \frac{p}{2}) \Psi_i(k; p) S^{-1}(k - \frac{p}{2}) \right\} \\ &= e_u \int \int \frac{d^4 k d^4 k'}{(2\pi)^8} \bar{\Psi}_{f,\rho}(k'; p+q) \left[ V(k', k + \frac{q}{2}) - V(k' - \frac{q}{2}, k) \right] \Psi_{i,\sigma}(k; p), \end{aligned} \quad (3.3a)$$

and

$$\begin{aligned} q_\mu \langle J_d^\mu \rangle &= -e_d \int \int \frac{d^4 k d^4 k'}{(2\pi)^8} \bar{\Psi}_{f,\rho}(k'; p+q) \left[ V(k' + \frac{q}{2}, k) - V(k', k - \frac{q}{2}) \right] \Psi_{i,\sigma}(k; p). \end{aligned} \quad (3.3b)$$

The wave equation eq (2.4) is used to obtain the last equality in eq (3.3a). The divergence of the one-body current is not generally zero, and the presence of a two-body current is required to conserve the electromagnetic current,

$$q_\mu \langle J_u^\mu + J_d^\mu + J_{int}^\mu \rangle = 0. \quad (3.4)$$

Thus, from eqs. (3.3) and (3.4), we get a very general restriction on the divergence of the relativistic two-body current operators. Specifically,

$$\begin{aligned} q_\mu J_{int}^\mu(k', k; [p, q]) &= e_u \left[ V(k' - \frac{q}{2}, k) - V(k', k + \frac{q}{2}) \right] \\ &\quad + e_d \left[ V(k' + \frac{q}{2}, k) - V(k', k - \frac{q}{2}) \right], \end{aligned} \quad (3.5)$$

where the charge of the  $\bar{d}$  quark is  $e_{\bar{d}} = -e_d$ .

Now, we derive the two-body current operator itself, *not* the divergence. An analytical derivation is possible when employing a separable interaction, which is a product of two form factors depending on the momenta of the charged particles. In the coordinate representation, the separable interaction can be written

$$V_{\alpha\beta;\delta\gamma}(x'_1, x'_2; x_1, x_2) = \Delta_{\alpha\beta}(x'_1, x'_2) \bar{\Delta}_{\delta\gamma}(x_1, x_2), \quad (3.6)$$

where

$$\Delta_{\alpha\beta}(x'_1, x'_2) = \int \int \frac{d^4 k'_1 d^4 k'_2}{(2\pi)^8} f(|k_1 - k_2|^2) \Omega_{\alpha\beta} e^{i k'_1 x'_1} e^{i k'_2 x'_2}, \quad (3.7)$$

Here the matrix  $\Omega$  is independent of momentum, and  $\Omega_{\alpha\beta} = \gamma_{\alpha\beta}^5$  for the pion. The form factor  $f(|k_1 - k_2|^2)$  depends on the momentum  $k_1(k_2)$  of the charged particle (2), and we introduce the photon field  $A^\mu(x)$  into this momentum dependence by minimal substitution<sup>14</sup>. This induces a change of the form factor,  $f(|k_1 - k_2|^2) \rightarrow f(|\bar{\partial}_1 - \bar{\partial}_2|^2)$ , where  $\bar{\partial}_i^\mu = \partial_i^\mu - ie_i A^\mu(x)$ . Thus the vertex  $\Delta(x_1, x_2)$  is modified by the photon field. The change in the vertex,  $\delta\Delta$  (Fig.10), is

$$\delta\Delta_{\alpha\beta}(x_1, x_2) = \int \int \frac{d^4 k_1 d^4 k_2}{(2\pi)^8} \left\{ f(|\bar{\partial}_1 - \bar{\partial}_2|^2) - f(|\partial_1 - \partial_2|^2) \right\} \Omega_{\alpha\beta} e^{ik_1 x_1} e^{ik_2 x_2}, \quad (3.8)$$

which is a function of the photon field operator  $A(x)$ .

The two-body electromagnetic current is obtained by taking the matrix elements for the photon annihilation process,  $J_{int}^\mu(x'_1, x'_2; x_1, x_2; q) = -(2\pi)^4 \langle 0 | \delta V | a_\mu^\dagger(q) \rangle$ , where the modified action induced by the photon field is given by

$$\delta V(x'_1, x'_2; x_1, x_2) = \delta\Delta(x'_1, x'_2) \cdot \bar{\Delta}(x_1, x_2) + \Delta(x'_1, x'_2) \cdot \delta\bar{\Delta}(x_1, x_2). \quad (3.10)$$

We refer to the Ref. 16 for further details. The results for this relativistic two-body current operator can be expressed in terms of the two-body interaction (Fig.11),

$$J_{int}^\mu(k', k; \{p, q\}) = -e_1 \frac{K_+^\mu}{K_+ \cdot q} \left[ V(k', k + \frac{q}{2}) - V(k', k) \right] + e_1 \frac{K_-^\mu}{K_- \cdot q} \left[ V(k' - \frac{q}{2}, k) - V(k', k) \right] \\ + \\ -e_2 \frac{K_+^\mu}{K_+ \cdot q} \left[ V(k', k - \frac{q}{2}) - V(k', k) \right] + e_2 \frac{K_-^\mu}{K_- \cdot q} \left[ V(k' + \frac{q}{2}, k) - V(k', k) \right]. \quad (3.11)$$

Here  $K_\pm^\mu = 2k'_\pm - 2k'_\pm \pm q$  (and similarly for the unprimed variables), and  $e_1(e_2)$  is the charge of  $u(\bar{d})$  quark. Note that this operator satisfies the general constraint given in eq (3.5).

## B. Matrix Elements

The Bethe-Salpeter equation and the interaction current operators are explicitly covariant in our approach, and the evaluation of the matrix elements should not depend on the frame we use; thus we choose the Breit frame

$$p^\mu = \frac{1}{2}(P - q)^\mu = (E, -\alpha\mathbf{q}), \\ p'^\mu = \frac{1}{2}(P + q)^\mu = (E, [1 - \alpha]\mathbf{q}), \\ q^\mu = (0, \mathbf{q}), \\ P^\mu = (2E, [1 - 2\alpha]\mathbf{q}), \quad (3.12)$$

where  $p^\mu$  and  $p'^\mu$  are momenta of the initial and final state of the bound state, and  $\alpha$  is given by  $E = \sqrt{\mu_i^2 + \alpha^2 q^2} = \sqrt{\mu_f^2 + (1 - \alpha)^2 q^2}$ . [When  $\mu_i = \mu_f = m_\pi$ ,  $\alpha = \frac{1}{2}$ .] In the Breit frame the interaction current can be expressed

$$J_{int}^\mu(k', k; q) = -e_u \left( \frac{\xi^\mu}{\xi \cdot q} [V(k', k + \frac{q}{2}) - V(k', k)] - \frac{\xi'^\mu}{\xi' \cdot q} [V(k' - \frac{q}{2}, k) - V(k', k)] \right) \\ + (e_d \text{ term}), \quad (3.13)$$

where  $\xi_\mu = \frac{(k+k')_\mu}{(k+k') \cdot q}$  and  $\xi'_\mu = \frac{(k+k')_\mu}{(k+k') \cdot q}$ . The matrix element (Fig.2) is given by

$$\langle J_{int}^\mu(q) \rangle = \int \frac{d^4 k'}{(2\pi)^4} \int \frac{d^4 k}{(2\pi)^4} \left\{ J_{int}^\mu \right\}, \quad (3.14)$$

where

$$\left\{ J_{int}^\mu \right\} = \{ S(k' - \frac{p'}{2}) \bar{\Gamma}(k') S(k' + \frac{p'}{2}) \}_{\beta\alpha} J_{int}^\mu(k', k; q)_{\alpha\beta\delta\epsilon} \{ S(k + \frac{p}{2}) \Gamma(k) S(k - \frac{p}{2}) \}_{\gamma\delta},$$

and the contribution to the charge form factor is given by  $\delta F_{int}(q^2) = |p' + p|^\mu \langle J_{int}^\mu(q) \rangle$ .

The numerical results are plotted in Fig. 12 for (a) the impulse form factor and (b) the correction from the interaction current. The best parameters obtained in the previous section ( $m_\rho = 248 \text{ MeV}$  and  $\Lambda = 450 \text{ MeV}$ ) are used, and the sensitivity to a variation of  $\Lambda$  is shown. The effect of the interaction current is zero at  $q^2 = 0$ , so the interaction current does not renormalize the charge. The relative size of the interaction current increases at large- $Q^2$ ,  $Q^2 > 4 \text{ GeV}^2$ , where the impulse form factor dies off. The comparison with the experimental data is shown in Fig. 13.

#### IV. Vector Meson Processes at space-like momentum transfer

In  $e^+e^-$ -collisions<sup>35</sup> the intermediate photon has time-like momentum ( $q^2 > 0$ ), where the Vector Meson Dominance (VMD) model works extremely well in predicting the cross sections of hadron production<sup>36</sup>, such as  $e^+e^- \rightarrow \pi^+\pi^-$ . Here, the strengths of rho-photon ( $f_\rho$ ) and rho-pion ( $g_{\rho\pi\pi}$ ) couplings are the fundamental parameters fixed from the decay processes of the physical rho meson,  $\rho \rightarrow e^+e^-$  and  $\rho \rightarrow \pi^+\pi^-$ . The VMD model somehow works even in the space-like region for predicting the pion charge form factor and radius, where the on-shell values of the coupling constants  $f_\rho(q^2 = m_\rho^2)$  and  $g_{\rho\pi\pi}(q^2 = m_\rho^2)$  are used as an approximation. This approximation has been applied for other mesonic processes such as  $\rho\pi\gamma$  coupling<sup>37</sup> as well as the  $\gamma^*\pi^0 \rightarrow \gamma$  reaction<sup>38</sup>.

However, baryon form factors behave asymptotically like  $q^{-4}$ , and from this fact it is very clear that the validity of monopole behavior due to the VMD is not universal. If the success of the hadronic VMD model in the low momentum region is based on quark-meson duality, the mixed usage of the VMD model and a quark model may induce some double counting. Here we examine the effects of virtual vector meson processes based on quark degrees of freedom, not as an effective hadronic description, but by actually using the  $q\bar{q}$  scattering matrix in the vector channel (Fig.3). The momentum dependence of the rho-photon ( $f_\rho(q^2)$ ) and the rho-pion ( $g_{\rho\pi\pi}(q^2)$ ) couplings, which can be obtained from the bound state solution of the Bethe-Salpeter equation, are automatically included in this approach. The propagator of the interacting  $q\bar{q}$  pair is introduced through the use of the scattering matrix in the vector channel, which has a bound state pole at the  $\rho$ -

meson mass. This consistent calculation can be performed almost analytically by using the relativistic separable model for the  $q\bar{q}$  interaction. We estimate the corrections to the impulse calculation of the pion charge form factor which arise from the  $q\bar{q}$  interaction in the vector channel, and discuss electromagnetic gauge invariance in the presence of the hadronic corrections.

The minimal requirements on this model are to (1) reproduce the correct position of  $\rho$ -meson pole in the  $q\bar{q}$  propagator in the vector channel, (2) satisfy electromagnetic gauge invariance at the  $\rho\gamma$  coupling so that the photon mass remains zero, and (3) reproduce the on-shell values of coupling constants  $f_\rho(q^2 = m_\rho^2)$  and  $g_{\rho\pi\pi}(q^2 = m_\rho^2)$ .

#### A. Separable Interaction in the Vector Channel

We introduce a separable quark-antiquark interaction for the Lorenz vector and isovector channel of the following form,

$$V_{\alpha\beta;\delta\gamma}^\mu(k', k; p) = af(p^2)G_{\alpha\beta}^\mu(k'; p)g_{\mu\nu}G_{\delta\gamma}^\nu(k; p)I_{cs}I_{iv}. \quad (4.1)$$

Here,  $G_{\alpha\beta}^\mu(k; p)$  is a vector vertex depending on the relative ( $k$ ) and total ( $p$ ) momenta of the  $q\bar{q}$  pair, Fig.14, and  $a$  is the coupling constant. The projection operators for the color singlet and isovector states are denoted by  $I_{cs}$  and  $I_{iv}$ , respectively. A function,  $f(p^2)$ , multiplies the interaction, and will be discussed later. For the vector vertex we use the following specific form

$$G^\mu(k; p) = \frac{1}{D_\rho(k^2)} \left( \gamma^\mu - \frac{\not{k}p^\mu}{p^2} \right). \quad (4.2)$$

This vector vertex couples to the polarization vector,  $\epsilon_\mu(p, \lambda)$ , of the intermediate vector particle. The summation over the polarization states of this intermediate particle gives  $\sum_\lambda \epsilon^\mu(p, \lambda)\epsilon^{*\nu}(p, \lambda) = g^{\mu\nu} - p^\mu p^\nu / p^2$ , where, using the vertex eq (4.2), we see that the  $p^\mu p^\nu / p^2$  term does not contribute, giving the structure eq (4.1). It is shown later that use of the vector vertex form  $\left( \gamma^\mu - \frac{\not{k}p^\mu}{p^2} \right)$  results in a simple realization of electromagnetic

gauge invariance for the  $\rho\gamma$  coupling.

The Bethe-Salpeter equation for the bound state vertex is given by

$$\Gamma_{ab}^\mu(k; p) = i \int \frac{d^4 k'}{(2\pi)^4} V_{ab,dc}^\rho(k, k'; p) S_{ca'}(k' + \frac{p}{2}) \Gamma_{a'b'}^\mu(k'; p) S_{b'd}(k' - \frac{p}{2}). \quad (4.3)$$

The solution can be written in terms of the vector vertex  $G^\mu(k; p)$ ,

$$\Gamma_{ab}^\mu(k; p) = \mathcal{N}_\rho G_{ab}^\mu(k; p) \chi_c \chi_f, \quad (4.4)$$

where  $\mathcal{N}_\rho$  is the normalization constant. Introducing the function  $\Pi(p^2)$  (see Fig. 15)

$$\Pi(p^2) = ia f(p^2) \int \frac{d^4 k}{(2\pi)^4} \frac{4m^2 - 2k^2 + p^2}{D_\rho^2(k^2) [(k + \frac{p}{2})^2 - m^2] [(k - \frac{p}{2})^2 - m^2]}, \quad (4.5)$$

we obtain the eigenvalue condition

$$\Pi(m_\rho^2) = 1. \quad (4.6)$$

The Bethe-Salpeter equation for the scattering matrix  $M$  is given by

$$M_{\alpha\beta;\delta\gamma}(k, k'; p) = V_{\alpha\beta;\delta\gamma}(k, k'; p) + i \int \frac{d^4 k''}{(2\pi)^4} V_{\alpha\beta;\lambda\lambda}(k, k''; p) S_{\lambda\gamma}(k'' + \frac{p}{2}) S_{\rho\lambda}(k'' - \frac{p}{2}) M_{\gamma\rho;\delta\gamma}(k'', k'; p), \quad (4.7)$$

and the existence of a bound state means that  $M$  has a pole at  $p^2 = m_\rho^2$

$$M_{\alpha\beta;\delta\gamma}(k, k'; p) = \frac{\Gamma_{\alpha\beta}^\mu(k; p) g_{\mu\nu} \Gamma_{\delta\gamma}^\nu(k'; p)}{p^2 - m_\rho^2} + R_{\alpha\beta;\delta\gamma}(k, k'; p), \quad (4.8)$$

Here,  $R(k, k'; p)$  is regular at  $p^2 = m_\rho^2$ , and  $\Gamma^\mu(k; p)$  is the bound state vertex, eq (4.4). [In fact eq (4.3) can be derived by inserting the expression (4.8) into (4.7) and taking the residue at  $p^2 = m_\rho^2$ ]. Inserting the explicit form eq (4.4) into eq (4.8) we get

$$M(k, k'; p) = \frac{\mathcal{N}_\rho^2 G^\mu(k; p) g_{\mu\nu} \bar{G}^\nu(k'; p)}{p^2 - m_\rho^2} I_{cs} I_{iv} + R(k, k'; p), \quad (4.9)$$

where the Greek letters have been dropped for simplicity. Meanwhile, we can explicitly solve the Bethe-Salpeter equation (4.7) by using the separable interaction (4.1). After the chain summation, the solution is

$$M(k, k'; p) = a f(p^2) \frac{G^\mu(k; p) g_{\mu\nu} G^\nu(k'; p)}{1 - \Pi(p^2)} I_{cs} I_{iv}, \quad (4.10)$$

where  $\Pi(p^2)$  was defined in eq (4.5). Equation (4.7), the chain summation, and the analytic solution (4.10) are illustrated in Fig. 16. Expanding the denominator near the pole gives

$$M(k, k'; p) = a f(m_\rho^2) \frac{G^\mu(k; p) g_{\mu\nu} G^\nu(k'; p)}{1 - \Pi(m_\rho^2) - (p^2 - m_\rho^2) \left[ \frac{d\Pi(p^2)}{dp^2} \right]_{p^2=m_\rho^2}} I_{cs} I_{iv}, \quad (4.11)$$

Comparing with eq (4.9), and using the eigenvalue condition (4.6), gives an explicit form of the wave function normalization

$$\mathcal{N}_\rho^2 = -a f(m_\rho^2) \left[ \frac{d\Pi(p^2)}{dp^2} \right]_{p^2=m_\rho^2}^{-1}, \quad (4.12)$$

## B. Vector Meson processes and Electromagnetic gauge invariance.

Hadronic corrections to the photon propagator must satisfy electromagnetic gauge invariance in order to keep the photon mass zero. A perturbative calculation<sup>39</sup> of the hadronic  $(q\bar{q})$  loop corrections to the photon propagator, after suitable regularization, gives the gauge independent form  $[g^{\mu\nu} q^2 - q^\mu q^\nu]$ . On the other hand, effective hadronic models must add an additional contact term in order to maintain gauge invariance<sup>40,41</sup>. Our separable interaction model of the vector meson also satisfies gauge invariance when it couples to a photon, and the momentum dependence of the  $\rho\gamma$ -coupling is determined from the interaction. The renormalized charge in QED already includes the hadronic corrections through the empirical value of  $\frac{e}{f_\rho} = \frac{1}{137}$ , where the hadronic correction is estimated to be  $(e/f_\rho)^2 \sim 0.28\%$ <sup>41</sup> at the renormalization point where the square of the photon four momentum is zero. Thus, we will require that our model gives no further renormalization

of electromagnetic charge. The same argument is used in a simpler approach<sup>42</sup> where the  $\rho$ -meson is treated as an elementary field.

We start with a calculation of the hadronic loop correction to the photon self-energy tensor,  $t^{\mu\nu}(p^2)$ , Fig. 17a. Using the  $q\bar{q}$  scattering matrix eq (4.10), gives

$$\begin{aligned} t^{\mu\nu}(p^2) &= -i \int \frac{d^4 k}{(2\pi)^4} \int \frac{d^4 k'}{(2\pi)^4} \left[ S(k - \frac{p}{2})(Q_q \gamma^\mu) S(k + \frac{p}{2}) \right]_{\beta\alpha} M_{\alpha\beta;4\gamma}(k, k'; p) \left[ S(k' - \frac{p}{2})(Q_q \gamma^\nu) S(k' + \frac{p}{2}) \right]_{\gamma\delta} \\ &= \left( g^{\mu\nu} p^2 - p^\mu p^\nu \right) t(p^2), \end{aligned} \quad (4.13a)$$

which is gauge invariant because  $p_\mu t^{\mu\nu} = 0$ . Here,  $t(p^2)$  is given by

$$t(p^2) = i \frac{\Delta^2(p^2)}{1 - \Pi(p^2)} \frac{\alpha f(p^2)}{p^2} \left( \text{Tr} \{ Q_q \gamma_\mu \} \text{Tr} \{ \gamma_\mu \} \right)^2, \quad (4.13b)$$

and  $\Delta(p^2)$  is obtained from

$$\begin{aligned} \Delta^{\mu\nu}(p^2) &= \int \frac{d^4 k}{(2\pi)^4} \text{Tr} \left\{ \gamma^\mu S(k - \frac{p}{2}) G^\nu(k; p) S(k + \frac{p}{2}) \right\} \\ &= \left( g^{\mu\nu} - \frac{p^\mu p^\nu}{p^2} \right) \Delta(p^2) \\ &= \left( g^{\mu\nu} - \frac{p^\mu p^\nu}{p^2} \right) \int \frac{d^4 k}{(2\pi)^4} \frac{4m^2 - 2k^2 + p^2}{D_\rho(k^2) \left( [k - \frac{p}{2}]^2 - m^2 \right) \left( [k - \frac{p}{2}]^2 - m^2 \right)}. \end{aligned} \quad (4.13c)$$

The propagator of photon is modified by this loop correction

$$\begin{aligned} D^{\mu\nu}(p^2) &= D_0^{\mu\nu}(p^2) + D_0^{\mu\sigma}(p^2) t_{\sigma\lambda}(p^2) D^{\lambda\nu}(p^2) \\ &= D_0^{\mu\nu}(p^2) \frac{1}{1 - t(p^2)} \end{aligned} \quad (4.14)$$

where  $D_0^{\mu\nu}(p^2) = \frac{g^{\mu\nu}}{p^2 - m_\rho^2}$  is the renormalized QED photon propagator without hadronic corrections. Here, it is important that  $t(p^2)$  has no pole at  $p^2 = 0$ ; if it did then it would cancel the photon pole in  $D_0(p^2)$  and induce a new pole in  $D$  at  $p^2 \neq 0$ , which would shift the photon mass from zero. This is the reason that we introduced the function  $f(p^2)$ , which is now chosen so that  $f(p^2)/p^2$  is regular at  $p^2 = 0$ . The simplest choice, which will be used from now on, is  $f(p^2) = p^2/m_\rho^2$ . Since the hadronic correction, which is finite at  $p^2 = 0$ , should be included in the renormalized charge, we write eq (4.14) as

$$\begin{aligned} D^{\mu\nu}(p^2) &= D_0^{\mu\nu}(p^2) Z^H(p^2) \\ &= D_0^{\mu\nu}(p^2) Z^H(0) \left[ 1 + \frac{Z^H(p^2) - Z^H(0)}{Z^H(0)} \right], \end{aligned} \quad (4.15)$$

where  $Z^H(p^2) = \frac{1}{1 - t(p^2)}$ , and the overall factor  $Z^H(0)$  is absorbed into the physical charge. The remaining hadronic correction  $\delta^H(p^2) \equiv \frac{Z^H(p^2) - Z^H(0)}{Z^H(0)} = \frac{t(p^2) - t(0)}{1 - t(p^2)}$  is zero at  $p^2 = 0$ .

The  $\rho\gamma$  coupling  $\kappa_\rho(p^2)$ , where  $(em_\rho^2/f_\rho)^2 \equiv \kappa_\rho^2(m_\rho^2)$  with  $\frac{f_\rho}{f_\pi} = 2.2 \pm 0.2^{41}$ , can be obtained by equating the quark loop diagram, Fig. 17a, with the effective hadronic diagram Fig. 17b:

$$\frac{\kappa_\rho^2(p^2)}{p^2 - m_\rho^2 + im_\rho \Gamma(p^2)} = \nu p^2 t(p^2), \quad (4.16)$$

Expanding the factor  $1 - \Pi(p^2)$  appearing in  $t(p^2)$  at  $p^2 = m_\rho^2$ , we get

$$\kappa_\rho^2(m_\rho^2) = N_\rho^2 \Delta^2(m_\rho^2) \left( \text{Tr} \{ Q_q \chi_f \} \text{Tr} \{ \chi_c \} \right)^2, \quad (4.17)$$

where  $\chi_f = \frac{1}{\sqrt{2}} \tau^3$ . Here we ignore the imaginary part of the vector meson propagator, which is mostly accounted by the  $\rho^0 \rightarrow \pi^+ \pi^-$  process not included in this diagram. Alternatively, a simple evaluation of the  $\rho^0 \gamma$  diagram, Fig. 18a, results in the same conclusion as eq (4.17).

### C. Vector Meson Contributions to the Pion charge form factor.

We first calculate the additional contributions to the quark current due to vector meson processes, which will be denoted  $J_{fV}^\mu$ . These processes arise from  $q\bar{q}$  scattering in the vector channel. Using the scattering matrix to describe this physics, as shown in Fig. 19, gives

$$J_{fV}^\mu(k; p)_{\alpha\beta} = \int \frac{d^4 k'}{(2\pi)^4} M_{\alpha\beta; \delta\gamma}(k, k'; p) \left[ S_i k' + \frac{p}{2} \right] (Q_\delta \gamma^\mu) S(k' - \frac{p}{2}) \Big|_{\gamma\delta} \quad (4.18)$$

Using the quantities defined in eq (4.5) and eq (4.13) gives the expression

$$J_{fV}^\mu(k; p) = \eta \frac{af(p^2)\Delta(p^2)}{1 - \Pi(p^2)} G^\mu(k; p), \quad (4.19)$$

where  $\eta = \chi_{fV} \otimes \chi_c \times \text{Tr}\{Q_\delta \chi_{fV}\} \text{Tr}\{\chi_c\}$  with  $\text{Tr}\{\chi_c\} = \sqrt{n_c}$  and  $\text{Tr}\{Q_\delta \chi_{fV}\} = e/\sqrt{2}$ . This is the isovector correction, which is necessarily important in the pion charge form factor. [For completeness, the isoscalar correction, needed later, will be given by simply assuming the universality of the separable interaction. Then, the expression of the isoscalar correction ( $J_{fS}^\mu$ ) is obtained by replacing  $\chi_{fV}$  and  $\text{Tr}\{Q_\delta \chi_{fV}\}$  by  $\chi_{fS}$  and  $\text{Tr}\{Q_\delta \chi_{fS}\} = \frac{1}{3} \text{Tr}\{Q_\delta \chi_{fV}\}$  in eq (4.19).] The correction to the pion charge form factor can be obtained by calculating the diagrams shown in Fig. 20, and the transition amplitude is given by

$$\mathcal{J}_\pi^\mu = -i \int \frac{d^4 k}{(2\pi)^4} \text{Tr} \left\{ \bar{\Gamma}_\pi(K'; p') S(k+p') J_{fV}^\mu(Q; q) S(k+p) \Gamma_\pi(K; p) S(k) \right\}, \quad (4.20)$$

where  $K' \equiv k + \frac{p'}{2}$  and  $K \equiv k + \frac{p}{2}$  are the  $q\bar{q}$  relative momenta in the final and initial states of pion, and  $Q \equiv k + \frac{p+p'}{2}$ . Further evaluation can be carried out in the Breit frame, eq (3.12). Including the  $\bar{d}$  process, we have the total correction to the pion charge form factor

$$\delta F_V(q^2) = C(q^2) T(q^2), \quad (4.21)$$

where

$$T(q^2) = \int \frac{d^4 k}{(2\pi)^4} \frac{(m^2 + p' \cdot p - k^2) \frac{k \cdot p}{p^2} + (m^2 - k^2 - \frac{k \cdot p}{2})}{D_\pi(K'^2) D_\pi(K^2) D_\rho(Q^2) ([k+p']^2 - m^2) ([k+p]^2 - m^2)},$$

$$C(q^2) = -4i \mathcal{N}_\pi^2 \frac{af(q^2)\Delta(q^2)}{1 - \Pi(q^2)},$$

and each factor is illustrated in Fig. 20.

The effective  $\rho^0 \rightarrow \pi^+ \pi^-$  vertex can be obtained from  $\mathcal{L}_{\rho\pi\pi} = f_{\rho\pi\pi} [p_1 - p_2]_\mu \epsilon^\mu(q, \lambda)$ , where  $p_1, p_2$  and  $q = p_1 + p_2$  are the momenta of  $\pi^+, \pi^-$  and  $\rho^0$ , and  $\epsilon^\mu(q, \lambda)$  is the polarization vector of  $\rho$ -meson. The coupling strength  $f_{\rho\pi\pi}$  is fitted to the width for the decay of a physical  $\rho$ -meson into  $\pi^+ \pi^-$ ,

$$\Gamma_{\rho \rightarrow \pi^+ \pi^-} = \frac{f_{\rho\pi\pi}^2 m_\rho}{4\pi \cdot 12} \left(1 - \frac{4m_\pi^2}{m_\rho^2}\right)^{\frac{3}{2}}. \quad (4.22)$$

By using our model for the vector meson vertex function  $\Gamma^\mu(k; p)$ , given by eq (4.4), we can calculate  $f_{\rho\pi\pi}(q^2)$  from the triangle diagrams of Fig. 18b. The transition amplitude is given by  $\Gamma_{\rho\pi\pi} = \Gamma_{\rho\pi\pi}^1 + \Gamma_{\rho\pi\pi}^2$ , where

$$\begin{aligned} \Gamma_{\rho\pi\pi}^1 &= \int \frac{d^4 k}{(2\pi)^4} \text{Tr} \left\{ \bar{\Gamma}_\pi(k - \frac{p_1}{2}; p_2) S(k - \frac{p_1 - p_2}{2}) \bar{\Gamma}_\pi(k + \frac{p_2}{2}; p_1) S(k + \frac{q}{2}) \Gamma_\rho(k; q) S(k - \frac{q}{2}) \right\}, \\ &= \mathcal{N}_\pi^2 \mathcal{N}_\rho \text{Tr} \{ \chi_{\pi^-}^\dagger \chi_{\pi^+}^\dagger \chi_{\rho^0} \} \text{Tr} \{ \chi_c^\dagger \} \mathcal{I}_{\rho\pi\pi}(p_1^2, p_2^2, p_1 \cdot p_2), \end{aligned} \quad (4.23)$$

and  $\Gamma_{\rho\pi\pi}^2 = \Gamma_{\rho\pi\pi}^1 (1 \leftrightarrow 2)$ . The loop integral  $\mathcal{I}_{\rho\pi\pi}$  is given by

$$\begin{aligned} \mathcal{I}_{\rho\pi\pi}(p_1^2, p_2^2, p_1 \cdot p_2) &= \\ &= \int \frac{d^4 k}{(2\pi)^4} \frac{\text{Tr} \left\{ \gamma^5 (\not{k} - \frac{p_1 - p_2}{2} + m) \gamma^5 (\not{k} + \frac{q}{2} + m) (\gamma^\mu - \frac{q^\mu}{q^2}) (\not{k} - \frac{q}{2} + m) \right\}}{D_\pi([k - \frac{p_1}{2}]^2) D_\pi([k + \frac{p_2}{2}]^2) D_\rho(k^2) ([k - \frac{p_1 - p_2}{2}]^2 - m^2) ([k + \frac{q}{2}]^2 - m^2) ([k - \frac{q}{2}]^2 - m^2)} \end{aligned}$$

#### D. Numerical Results.

The expression for the vector meson corrections, eq (4.21), has quite an involved structure with many denominators in the integrand. Nevertheless, we can in principle evaluate the integral as accurately as necessary by standard numerical methods since the photon is space-like and no singularity is involved. We first express this momentum integral in terms of Feynman parameters, which has the structure

$$\int \cdots \int \prod_{i=1}^L dx_i \delta(\sum_{j=1}^L x_j - 1) F(x_1, \cdots, x_L) .$$

We can then perform the numerical integration by the Monte-Carlo method. The delta function constraint is handled by doing the integration on the surface of a  $L$ -dimensional hypersphere.

When we evaluate the  $\rho\gamma$ -coupling, we face an integral given by eq (4.13c). In order for the integral to be finite, the momentum distribution  $D_\rho(k^2)$  is required to behave like  $k^{2N}$  with  $N \geq 2$ . We therefore choose  $D_\rho$  to be a product of monopole functions

$$D_\rho(k^2) = (k^2 - \Lambda_{\rho 1}^2)(k^2 - \Lambda_{\rho 2}^2), \quad (4.24)$$

with two parameters  $\Lambda_{\rho 1}$  and  $\Lambda_{\rho 2}$ . These parameters are fixed to give the empirical values of  $\rho\gamma$  and  $\rho\pi\pi$  coupling constants,  $f_\rho^2/4\pi = 2.2$  and  $g_{\rho\pi\pi}^2/4\pi = 2.3$ . By using the pion vertex, eq (2.4), we get  $\Lambda_{\rho 1} = 0.6 \sim 0.7\text{GeV}$  and  $\Lambda_{\rho 2} = 1.0\text{GeV}$  for  $m_\rho = 248\text{MeV}$ . Here, we assume  $m_\rho = 2m_\pi$ , in order to avoid the  $q\bar{q}$  threshold singularity which arises when calculating the  $\rho \rightarrow \pi\pi$  amplitude, and which is very difficult to calculate with the Monte-Carlo method. This approximation is used only for modeling the momentum distribution by estimating the sizes of  $\Lambda_{\rho 1}$  and  $\Lambda_{\rho 2}$ , and is not used in the calculation of  $\delta F_V(q^2)$ .

Figure 21 shows the numerical results for the vector meson corrections  $\delta F_V(q^2)$ , and compares them to the impulse contribution. Note that  $\delta F_V(q^2)$  is very small, but the contribution to the charge radius is not negligible. The Table shows each contribution to the charge radius.

The correction  $\delta F_V(q^2)$  is zero at  $q^2 = 0$ , and has a maximum contribution at  $Q^2 \sim 0.4\text{GeV}^2$ , the same qualitative conclusion found in other models<sup>43</sup>. In Fig. 22, we plot

$T(q^2)$  and  $C(q^2)$  defined by eq (4.21) and in Fig. 20. The  $Q^2$  dependence of  $T(q^2)$  is similar to the  $Q^2$  dependence of the impulse form factor, except for the additional damping effect caused by the  $q\bar{q}$  momentum distribution. The peak at  $q^2 = m_\rho^2$  in  $C(q^2)$  is caused by the  $\rho$ -meson pole in the scattering matrix, eq (4.11), and  $C(q^2)$  is zero at  $q^2 = 0$  so that the charge is not renormalized again. The peak in  $\delta F_V(q^2)$  can be understood from the product  $\delta F_V(q^2) = C(q^2)T(q^2)$ . The present model takes into account the  $q^2$ -dependence of the couplings  $f_\rho(q^2)$  and  $g_{\rho\pi\pi}(q^2)$ .

#### V. Summary, Discussion, and Predictions

We summarize the work presented in this paper:

(i) We introduced a relativistic separable interaction to model the chirally symmetric  $q\bar{q}$  interaction. We solved the Schwinger-Dyson equation for the quark self-energy, and the dynamical mass. In our model, the onset of chiral symmetry breaking is associated with the range and momentum dependence of the separable interaction. The pion field emerges as a Nambu-Goldstone boson associated with the symmetry breaking, and the Bethe-Salpeter equation is solved for the  $q\bar{q}$  momentum distribution of the pion.

(ii) Low energy observables (the pion weak decay constant, two-photon decay width and the charge radius) are calculated with an effective mass approximation to the dynamical quark mass. Choosing the effective quark mass,  $m_q = 248\text{MeV}$ , and pion momentum scale,  $\Lambda = 450\text{MeV}$ , results in excellent agreement with the experimental data. Here, we remark that the momentum distribution of the pion wave function plays the role of a momentum cutoff in our Feynman diagrams, and this effect depends on the number of pion vertices in the process. This is an essential difference from the original Nambu-Jona-Lasinio model, where some noncovariant momentum cutoff enters into all loop integrals.

(iii) We predict the charge form factor of the pion by calculating the impulse diagram, using the Bethe-Salpeter wave function to describe the pion structure. Excellent agreement with the experimental data is obtained with the parameters ( $m_q = 248\text{MeV}$  and  $\Lambda = 450\text{MeV}$ ).

(iv) In addition to the impulse diagram for the pion charge form factor, we evaluate

the effect of the two-body interaction currents associated with the relativistic separable interaction. This effect becomes important in the large  $Q^2$  region ( $Q^2 > 2GeV^2$ ), though its correction to the charge radius is negligible. This effect does not renormalize the charge of the pion.

(v) The separable  $q\bar{q}$  interaction model is then applied to the Lorentz vector channel. The Bethe-Salpeter equation for the scattering matrix is solved by the chain summation to yield a bound state pole at the  $\rho$ -meson mass. The resulting  $\rho$  channel scattering matrix is added to the impulse diagram for the charge form factor. This is a generalization of the Vector Meson Dominance model to space-like momentum transfers. The composite structures of the vector meson and pion are taken into account. The numerical results turn out to give a very small correction to the charge form factor of the pion; the maximum contribution, which occurs at  $Q^2 = 0.4GeV^2$ , is only about 5 ~ 8% of the impulse contribution. However, this effect makes a significant contribution to the charge radius. Because of electromagnetic gauge invariance, this vector meson process does not renormalize the charge.

We wish to emphasize that the additional vector meson processes have been found to be very small. By using a dynamical quark mass,  $m_q \sim 250MeV$ , and a  $q\bar{q}$  momentum distribution for the pion, we are able to reproduce the observables very well using only the impulse approximation, and without relying on effects from Vector Meson Dominance. A similar conclusion follows from the  $q\bar{q} \leftrightarrow$  meson duality<sup>44</sup>, even without the effect of quark confinement.

We now present two predictions of this model. Using the values of the parameters determined from the previous calculations, we calculate two new form factors in which the pion structure is involved.

First, we predict the transition form factor for the transition  $\gamma^*\pi^0 \rightarrow \gamma$ . While the axial anomaly gives a model independent explanation<sup>28,29,30</sup> of the real two-photon decay ( $\Gamma_{\pi^0 \rightarrow \gamma\gamma}$ ), if the one of photons ( $\gamma^*$ ) is virtual, its four-momentum  $Q^2$  becomes an additional dynamical variable which probes the dynamics of the axial anomaly. Using the same parameters, i.e  $m_q = 248MeV$  and  $\Lambda = 450MeV$ , Fig. 24 shows our prediction for this form factor, based on the diagram shown in Fig. 8. For comparison, the result of

the hadronic VMD model is also shown. Using the quark mass  $m_q = 248MeV$  results in excellent agreement, and the result is found to be sensitive to the size of the quark mass.

Finally, we predict the form factor for the  $\rho\pi\gamma$ -coupling. This coupling is particularly important in calculations of nuclear exchange currents at large momentum transfer. For example, a relativistic calculation of the deuteron form factor is sensitive to the  $\rho\pi\gamma$ -exchange current<sup>32</sup>. Our numerical results are shown in Fig.25, where the prediction with the hadronic VMD approach is also given for comparison. These different approaches agree with each other for  $Q^2 < 1GeV^2/c^2$ . However, the strengths are 40 ~ 50% different at  $Q^2 = 2 \sim 4GeV^2/c^2$ , where the  $\rho\pi\gamma$  coupling is most important in applications to the calculation of the deuteron form factor.

#### Acknowledgements

The work of H.I was supported by NSF grant RII-8704038, that of W.W.B was supported by NASA grant NAG-1-447 and RII-8704038, and that of F.G was supported in part by the Department of Energy through Grant Number DE-FG05-88ER40435. H.I would like to thank the Continuous Electron Beam Accelerator Facility (CEBAF) for hospitality. In particular, he appreciates the very useful and friendly discussions with members of CEBAF theory group.

## References

† Present address: Department of Physics, George Washington University, Washington DC 20052. Bitnet address: ITO@GWUVM

1. J. Goldstone, *Nuovo Cimento* **10**, 154 (1961)
2. F. E. Low, *Phys. Rev.* **90**, 1428 (1954); **110**, 974 (1958);  
M. Gell-Mann and M. L. Goldberger, *Phys. Rev.* **90**, 1433 (1954).
3. S. Adler and R. Dashen, "*Current Algebras*" (Benjamin, New York 1968);  
S. B. Treiman, "*Lecture on Current Algebra and Its Applications*" (Princeton University Press 1972).
4. S. O. Bäckmann, G. E. Brown and J. A. Niskanen, *Phys. Rep.* **124**, 1 (1985).
5. A. M. Bernstein and B. R. Holstein, MIT preprint 1991.
6. J. Cornwall, *Phys. Rev.* **D22**, 1452 (1980); A. Casher *Phys. Lett.* **83B**, 395 (1979); J. R. Finger and J. E. Mandula, *Nucl. Phys.* **B199**, 168 (1982).
7. Y. Nambu and G. Jona-Lasinio, *Phys. Rev.* **122**, 345 (1961); **124**, 246 (1961).
8. V. Bernard, *Phys. Rev.* **D34**, 1601 (1986);  
V. Bernard, U.-G. Meissner and I. Zahed, *Phys. Rev.* **D36**, 819 (1987);  
T. Hatsuda and T. Kunihiro, *Prog. Theor. Phys.* **74**, 765 (1985);
9. A. L. Fetter and J. D. Walecka: *Quantum Theory of Many-Particle Systems* (McGraw-Hill, New York, 1971).
10. J. Bardeen, L. N. Cooper and J. R. Schrieffer, *Phys. Rev.* **106**, 1175 (1957).
11. K. Higashijima, *Phys. Rev.* **D29**, 1228 (1984); K. Aoki, M. Bando,  
T. Kugo, M. G. Mitchard and H. Nakatani, *Prog. Theor. Phys.* **84**, 683 (1990).
12. K. Johnson, M. Baker and R. Willey, *Phys. Rev.* **130**, B1111 (1964);  
T. Maskawa and H. Nakajima, *Prog. Theor. Phys.* **52**, 1326 (1974);  
R. Fukuda and T. Kugo, *Nucl. Phys.* **B117**, 250 (1976).
13. H. D. Polizer, *Nucl. Phys.* **B117**, 397 (1976).
14. S. J. Brodsky and G. P. Lepage, *Phys. Rev.* **D24**, 1808 (1981); G. R. Farrar and  
D. R. Jackson, *Phys. Rev. Lett.* **43**, 246 (1979).
15. F. Gross and D. O. Riska, *Phys. Rev.* **C36**, 1928 (1987); R. M. Woloshyn,  
*Phys. Rev.* **C12**, 1901 (1975).
16. H. Ito, W. W. Buck and F. Gross, *Phys. Rev.* **C43**, 2483 (1991).
17. J. J. Sakurai, *Phys. Rev. Lett.* **22**, 981 (1969); J. J. Sakurai, *Phys. Lett.* **46B**,  
207 (1973).
18. R. K. Bhaduri "*Models of Nucleon*" Chapter 7 (Addison-Wesley Publishing  
1988), and the references therein.
19. R. A. Bertlmann, *Acta. Physica Austriaca* **53** 305 (1981).
20. M. Gell-Mann, R. Oakes and B. Renner, *Phys. Rev.* **175**, 2185 (1968); J. Gasser  
and H. Leutwyler, *Phys. Rep.* **87**, 77 (1982).
21. M. D. Scadron, *Ann. of Phys.* **148**, 257 (1983); M. D. Scadron,  
*Rep. Prog. Phys.* **44**, 213 (1981).
22. H. Pagels, *Phys. Rev.* **D7**, 3689 (1973); H. Pagels and S. Stokar,  
*Phys. Rev.* **D20**, 2947 (1979).
23. V. Bernard, R. Brockmann, M. Schaden, W. Weise and E. Werner  
*Nucl. Phys.* **A412**, 349 (1984).
24. R. T. Cahill and C. D. Roberts, *Phys. Rev.* **D32**, 2419 (1985).
25. W. Weise, "*Quarks and Nuclei*", edited by W. Weise (World Scientific 1984).
26. D. G. Caldi, *Phys. Rev. Lett.* **30**, 121 (1977); R. D. Carlitz, *Phys. Rev.* **D17**,  
3225 (1978); C. G. Callan, R. Dashen and D. J. Gross, *Phys. Rev.* **D17**,  
2717 (1978).
27. R. Haag and Th. A. J. Maris, *Phys. Rev.* **132**, 2325 (1963).
28. J. Steinberger, *Phys. Rev.* **70**, 1180 (1949); J. Schwinger, *Phys. Rev.* **82**,  
664 (1951); S. Adler, *Phys. Rev.* **177**, 2426 (1969);  
J. Bell and R. Jackiw, *Nuovo Cimento* **60A**, 47 (1969).
29. K. Fujikawa, *Phys. Rev. Lett.* **42**, 1195 (1979); *Phys. Rev.* **D21**, 2848 (1980).
30. R. J. Crewther, *Phys. Rev. Lett.* **28**, 1421 (1972).
31. M. Aguilar-Benitez *et al* (Particle Data Group), *Phys. Lett.* **170B**, 1 (1986).
32. E. B. Dally *et al*, *Phys. Rev. Lett.* **48**, 375 (1982).
33. E. Hunmel and J. A. Tjon, *Phys. Rev. Lett.* **63**, 1788 (1989).
34. K. Ohta, *Phys. Rev.* **C40**, 1335 (1989); **C41**, 1213 (1990).

35. F. E. Close and W. N. Cottingham, "*Electromagnetic interactions of Hadrons*", edited by A. Donnachie and G. Shaw ( Plenum Press 1978).
36. B. L. Ioffe, V. A. Khoze and L. N. Lipatov, "*Hard Processes*" ( North Holland Physics Publishing 1984).
37. M. Chemtob, E. Moniz and M. Rho, *Phys. Rev. C* **10**, 344 (1974).
38. H. J. Behrend *et al*(CELLO Collaboration), DESY preprint ISSN 0418-9833(1990).
39. J. D. Bjorken and S. D. Drell, *Relativistic Quantum Mechanics* (McGraw Hill 1964); L. H. Ryder, *Quantum Field Theory* (Cambridge University Press 1985).
40. N. M. Kroll, T. D. Lee and B. Zumino, *Phys. Rev.* **157**, 1376 (1967).
41. J. J. Sakurai, *Current and Meson* (University of Chicago press 1969).
42. V. Bernard and U.-G. Meissner, *Phys. Rev. Lett.* **61**, 2296 (1988).
43. G. V. Efimov and M. A. Ivanov, *International Journal of Modern Physics A* **4**, 2031 (1989).
44. J. J. Sakurai, K. Schilcher and M. D. Tran, *Phys. Lett.* **102B**, 55 (1981); J. S. Bell and J. Pasupathy, *Phys. Lett.* **83B**, 389 (1970).
45. C. J. Bebek *et al*, *Phys. Rev.* **D17**, 1893 (1978).

The pion charge radius obtained from various contributions.

**TABLE**

	Impulse	Impulse + Interaction Current	Impulse + Interaction Current + Vector Meson Process
$r_\pi [fm]$	0.740	0.754	0.853

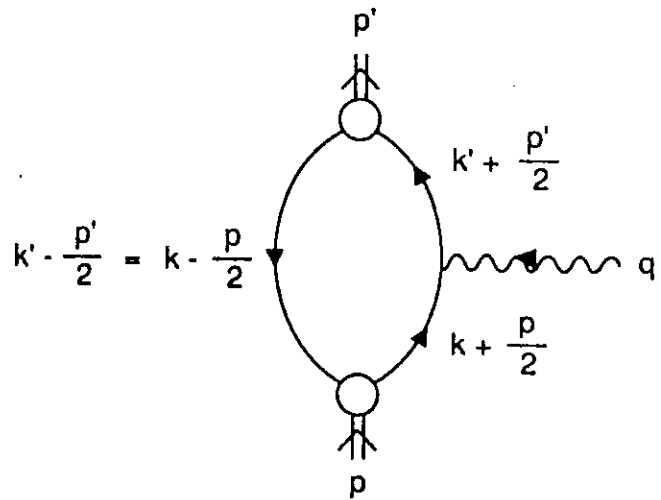


Fig. 1

An impulse diagram for the pion charge form factor, where the open circles are the Bethe-Salpeter vertex functions of the  $q\bar{q}$  pion. The solid lines are quark lines, and the wavy line is meant to be a photon with momentum  $q$ .

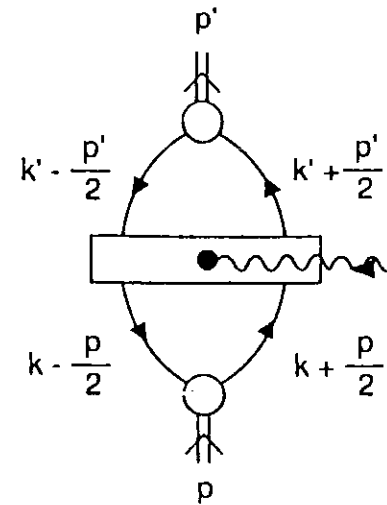


Fig. 2

The two-body interaction current diagram. The rectangular box is the relativistic two-body interaction current operator,  $J_{\mu\nu}^{\alpha}(k', k; [p, q])$ .

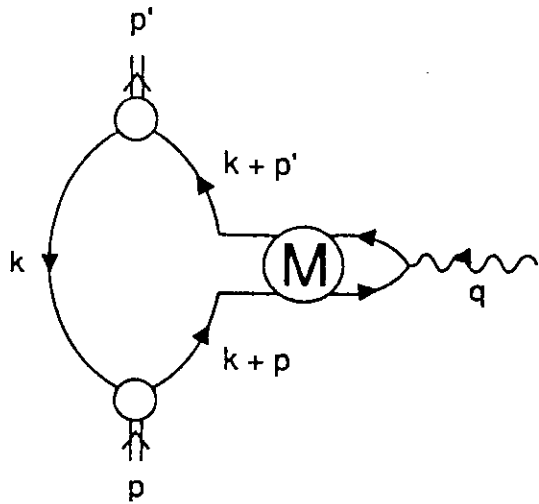


Fig. 3  
A diagram including the modification of a photon-quark coupling due to the vector meson process. The circle with  $M$  is the  $q\bar{q}$  scattering matrix in the Lorenz vector channel.

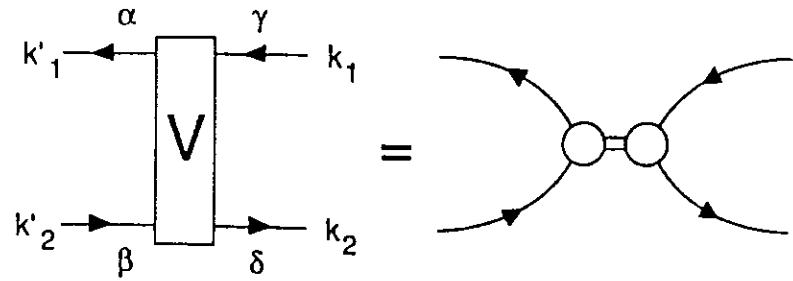


Fig. 4  
A relativistic separable interaction as a product of two nonlocal vertices indicated by the open circles.

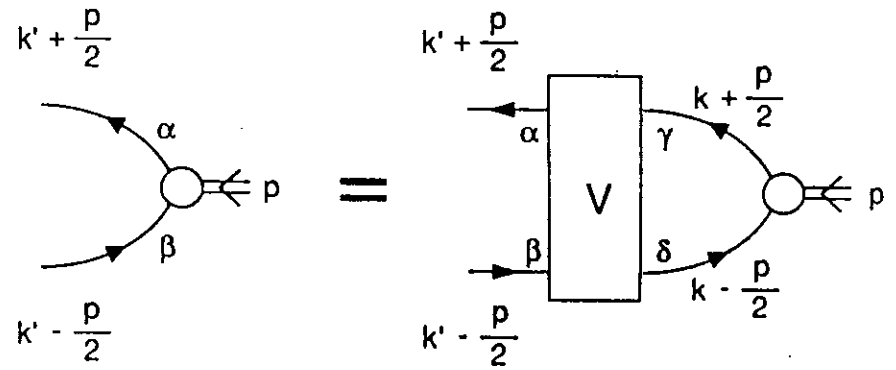


Fig. 5  
The Bethe-Salpeter equation for a bound state vertex, which is indicated by the open circle.

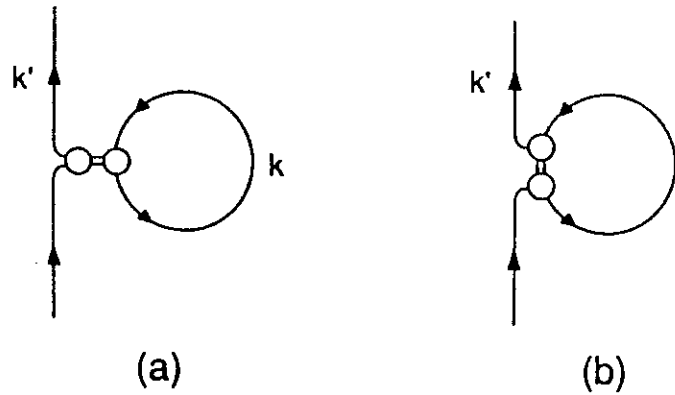


Fig. 6  
The diagrams for the quark self-energy induced by the separable interaction; (a) Hartree and (b) Fock terms.

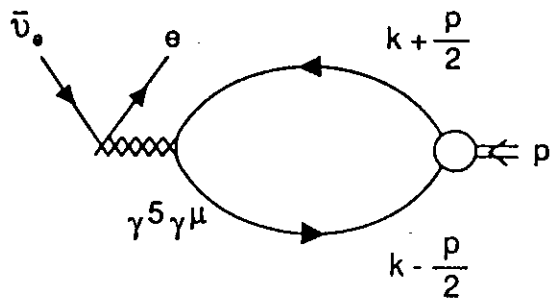


Fig. 7  
A diagram for the pion weak decay,  $\pi^- \rightarrow e^- + \bar{\nu}_e$ . The zigzag line is a weak vector boson,  $W^-$ .

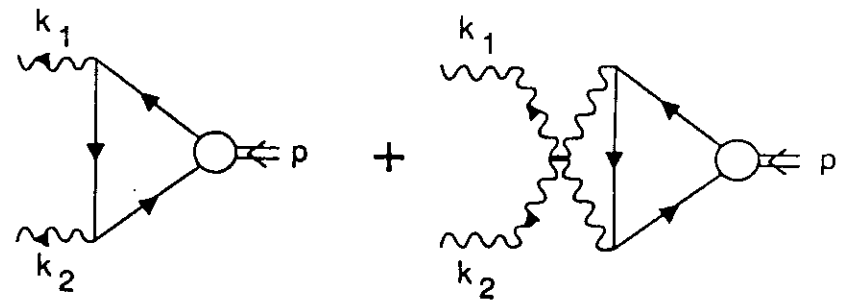


Fig. 8  
Diagrams for the fermion triangle axial anomaly, where the wavy lines are photons with the momentum  $k_1$  and  $k_2$ .

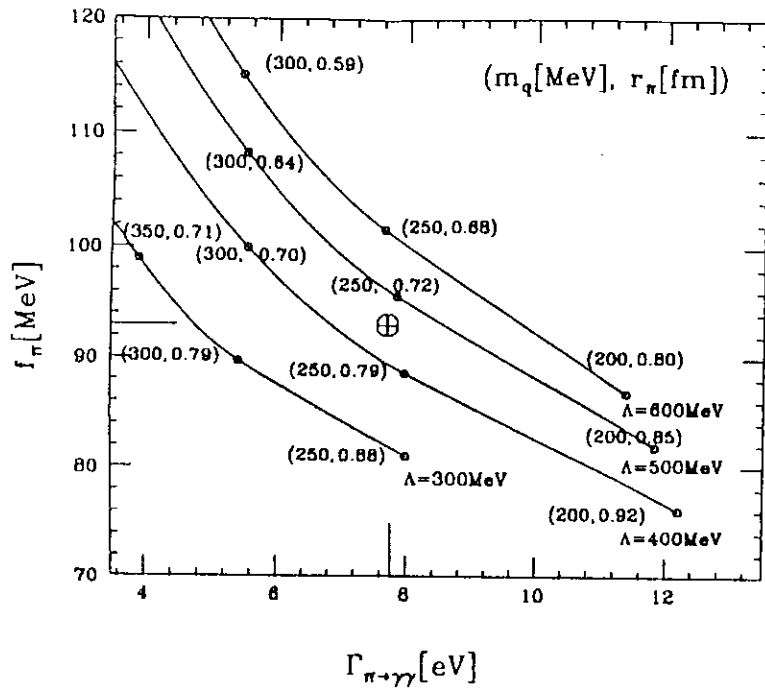


Fig. 9

The results for the low energy observables, the pion weak decay constant ( $f_\pi$ ), two-photon decay width ( $\Gamma_{\pi \rightarrow \gamma\gamma}$ ) and the charge radius ( $r_\pi$ ). The dependence on the effective quark mass ( $m_q$ ) and on the parameter of the separable interaction ( $\Lambda$ ) is shown. The circle with a cross is the best fit;  $m_q = 248 \text{ MeV}$  and  $\Lambda = 450 \text{ MeV}$ .

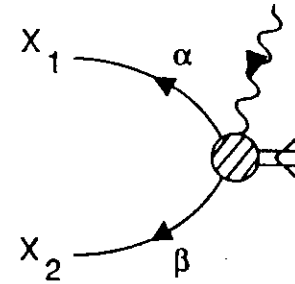


Fig. 10

The modified  $q\bar{q}-\pi$  vertex function (circle with hatching) due to minimal substitution of the photon field.

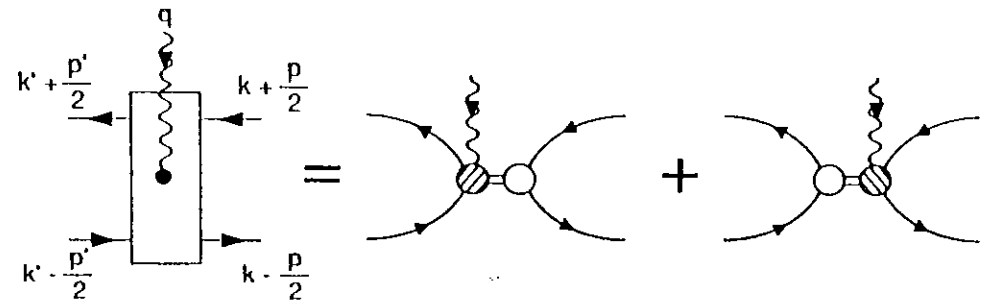


Fig. 11

The relativistic operator for the two-body interaction current, which is expressed in terms of products of the  $q\bar{q}-\pi$  vertex and its modification (Fig. 10) due to the photon field.

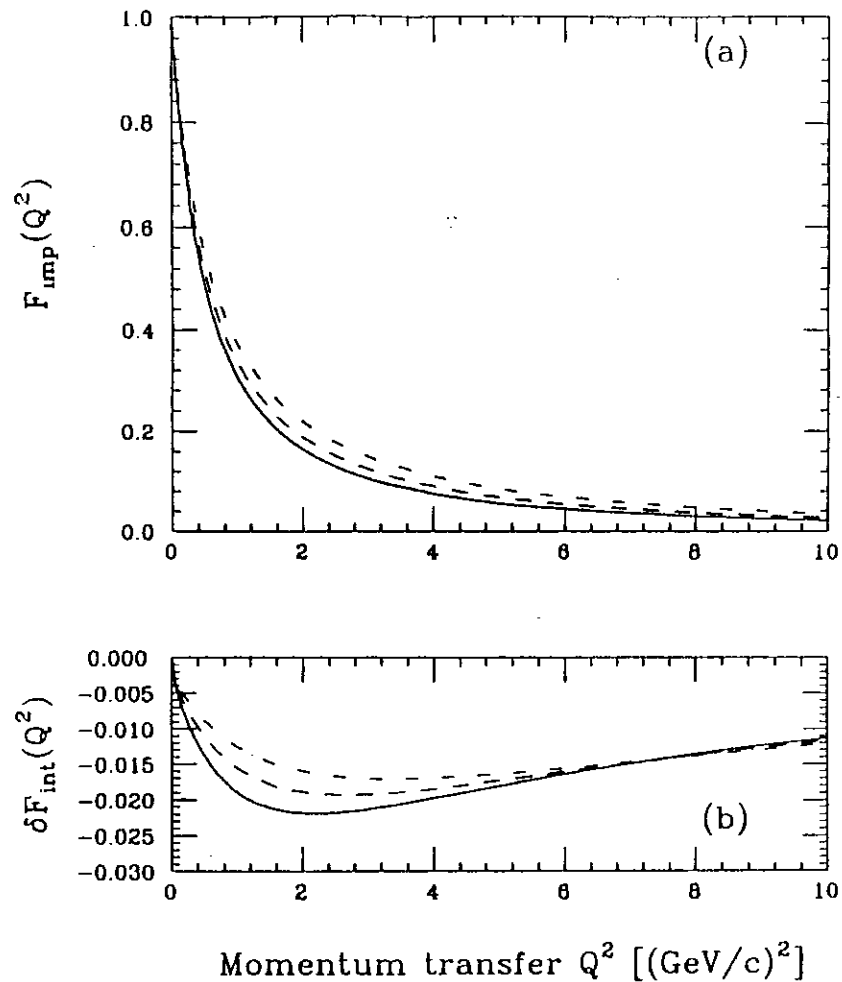


Fig. 12

Contributions of (a) the impulse ( $F_{\text{imp}}(Q^2)$ ) and (b) the interaction ( $\delta F_{\text{int}}(Q^2)$ ) form factors. The solid line is the result with  $m_\pi = 248 \text{ MeV}$  and  $\Lambda = 450 \text{ MeV}$ , the dashed (dash-dotted) line is the one with  $m_\pi = 248 \text{ MeV}$  and  $\Lambda = 550(650) \text{ MeV}$ .

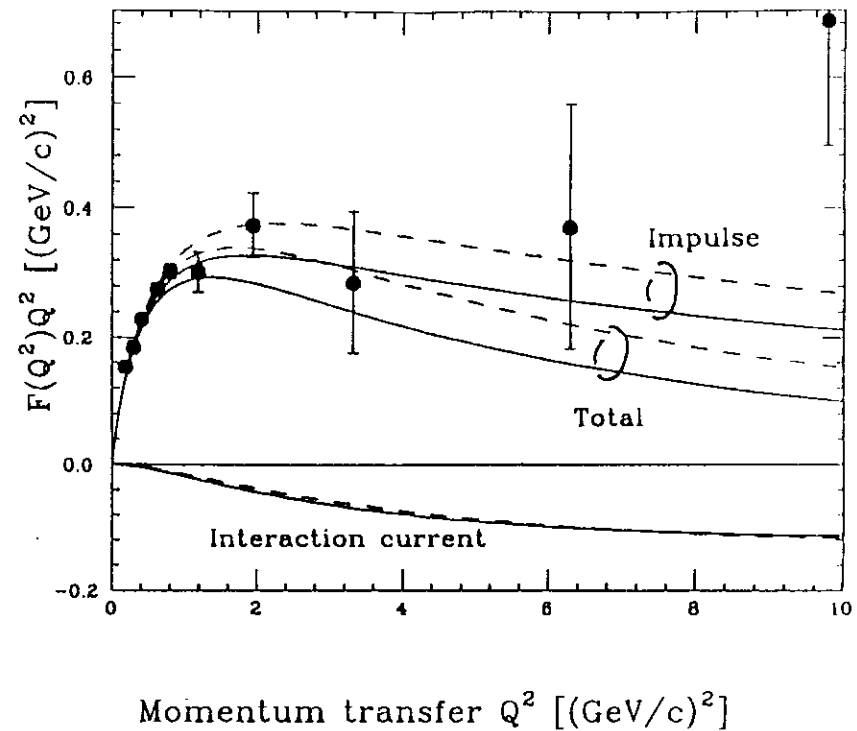


Fig. 13

The pion charge form factor multiplied by  $Q^2$ . Contributions of the impulse and the interaction form factors are shown and compared with the experimental data. The solid (dashed) line is the result with  $m_\pi = 248 \text{ MeV}$  and  $\Lambda = 450(550) \text{ MeV}$ . The experimental data are from Ref. 45.

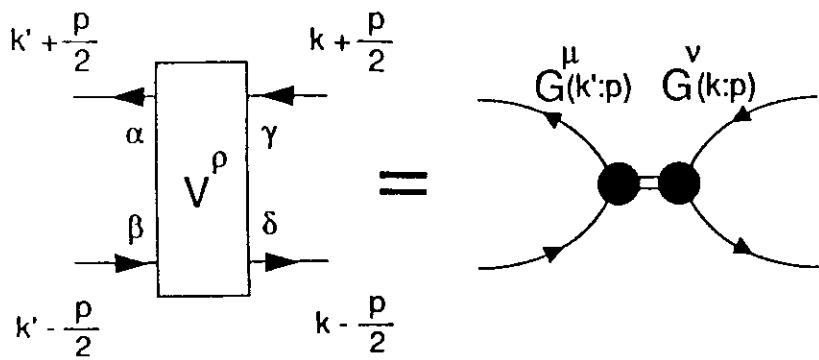


Fig. 14  
The separable interaction for the Lorenz vector channel, where the solid circle is the vector vertex  $G^\mu(k:p)$ .

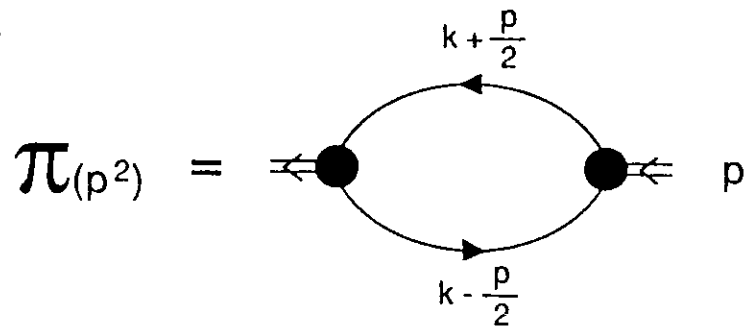


Fig. 15  
The vector meson self-energy loop expressed in terms of the Bethe-Salpeter vertex function.

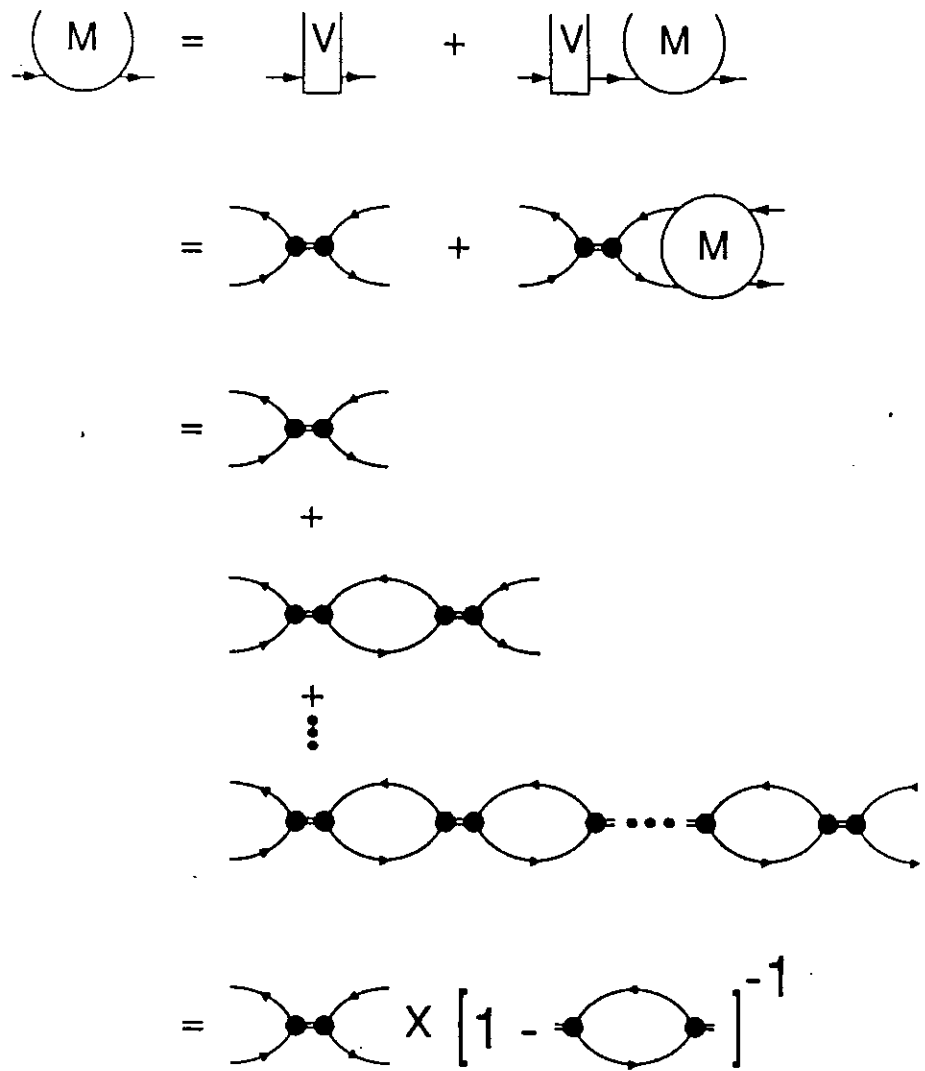


Fig. 16  
The integral equation for the  $q\bar{q}$  scattering matrix in the Lorenz vector channel. The chain summation is illustrated.

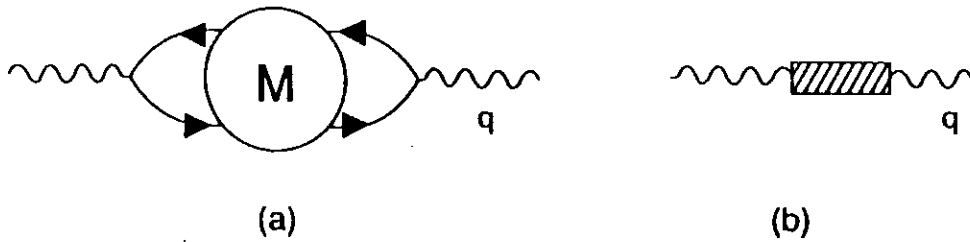


Fig. 17

Diagrams which give rise to the hadronic correction to the photon propagator. (a) Our model, in which the hadronic correction arises from the  $q\bar{q}$  scattering matrix. (b) Hadronic corrections from the Vector Meson Dominance model.

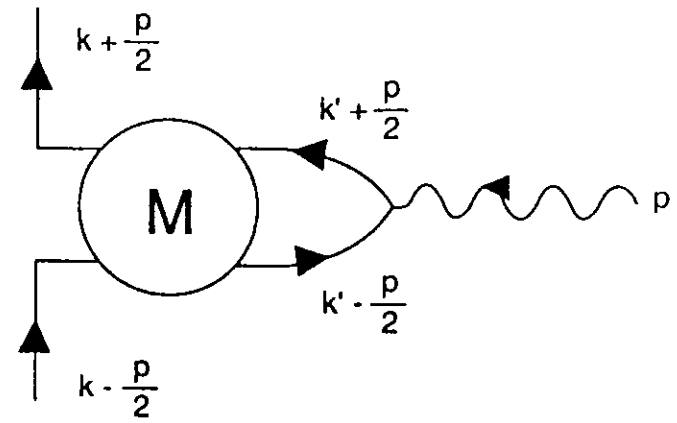


Fig. 19

Modified quark-charge operator with momentum transfer  $p$ . The circle with  $M$  is the  $q\bar{q}$  scattering matrix in the Lorenz vector channel, and the wavy line is a photon with momentum  $p$ .

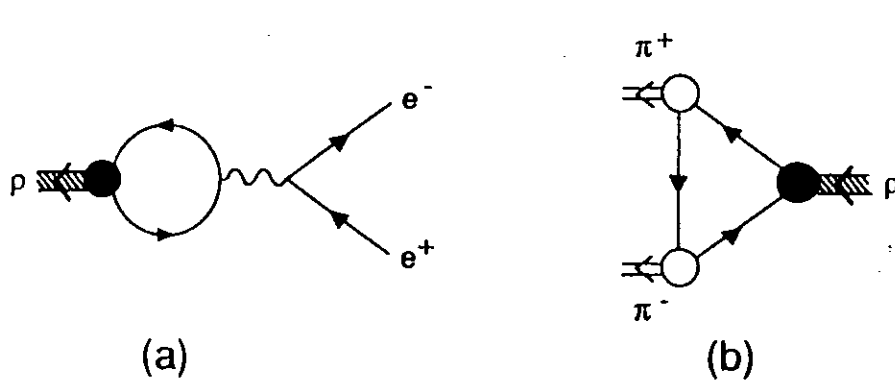


Fig. 18

Physical processes for on-shell  $\rho$ -meson decays. (a)  $\rho^0 \rightarrow e^+e^-$  and (b)  $\rho^0 \rightarrow \pi^+\pi^-$ .

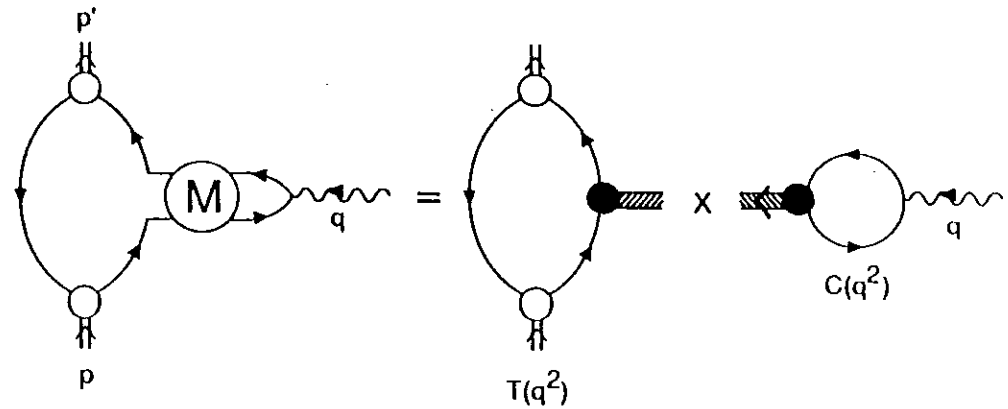


Fig. 20

The diagram for the pion charge form factor which includes the correction from the vector meson process. This diagram has two factors:  $T(q^2)$  from the  $\pi\pi$  vector vertex triangle diagram and  $C(q^2)$  from the  $\gamma$ -vector vertex coupling to the vector channel propagator.

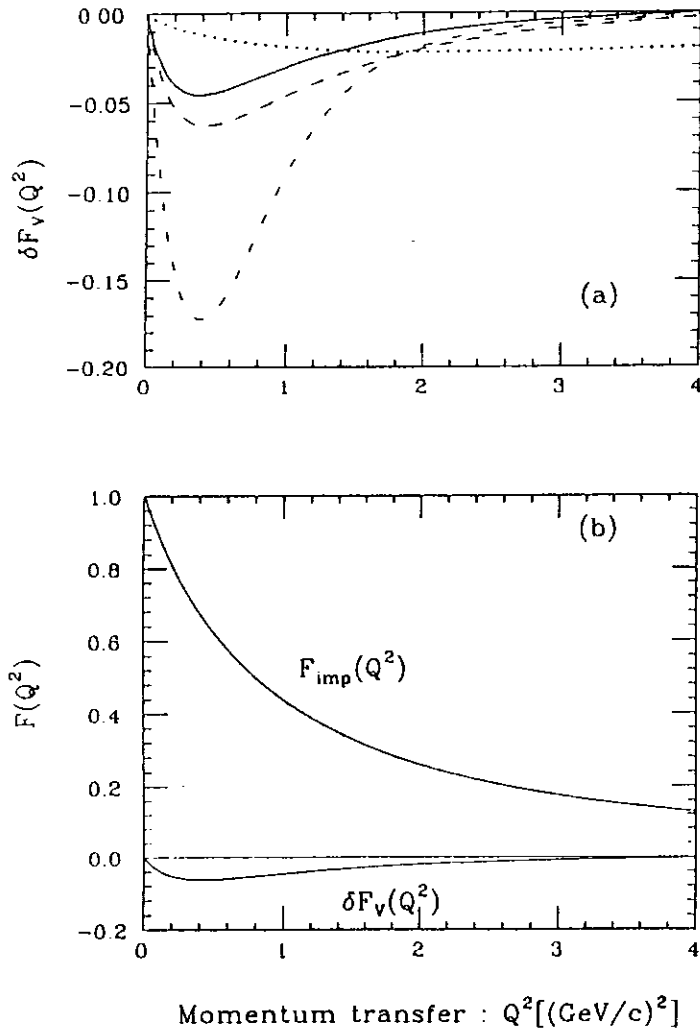


Fig. 21

The plots of the vector meson correction ( $\delta F_V(Q^2)$ ) to the pion charge form factor. (a) Our calculation is given by the solid line ( $\Lambda = 450 \text{ MeV}$ ) and the dashed line ( $\Lambda = 550 \text{ MeV}$ ). The results from the Quark Confining Model<sup>13</sup> are given by the dot-dash line. The effect of the interaction current  $\delta F_{\text{int}}(Q^2)$  is given (dotted line) for comparison. (b) This figure shows the relative size of the contributions from the impulse and the vector meson process.

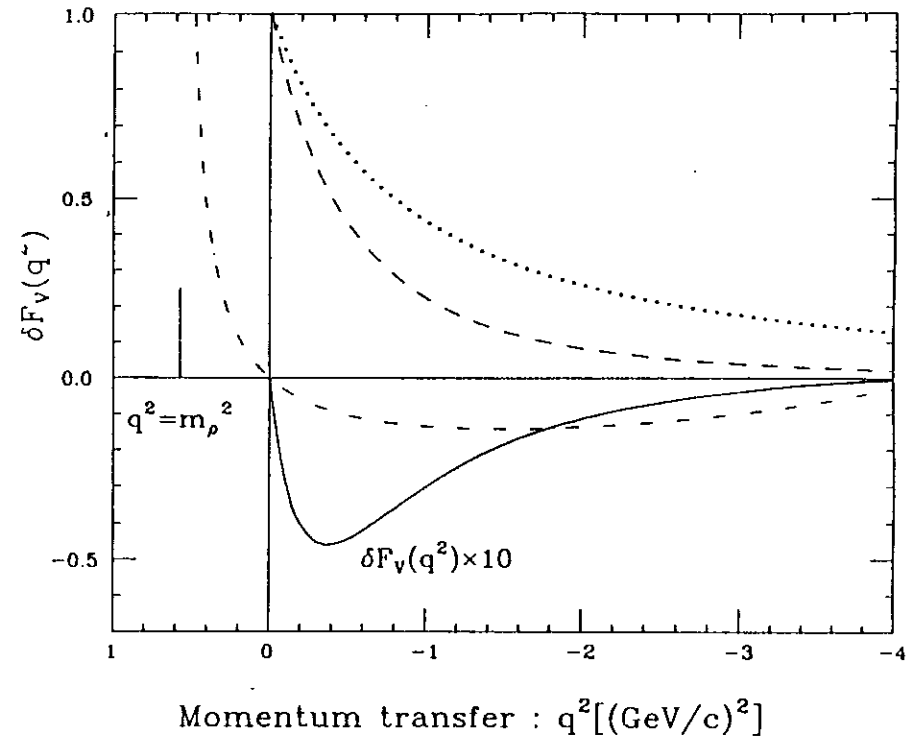


Fig. 22

Plot of the different factors,  $T(q^2)$  and  $C(q^2)$ , defined in Fig. 20. The dash line is the factor  $T(q^2)$  and the dot-dash line is the factor  $C(q^2)$ . The total,  $\delta F_V(q^2) \times 10$ , is the solid line. For comparison, the dotted line shows the impulse form factor calculated from the  $\pi\pi\gamma$  triangle diagram.

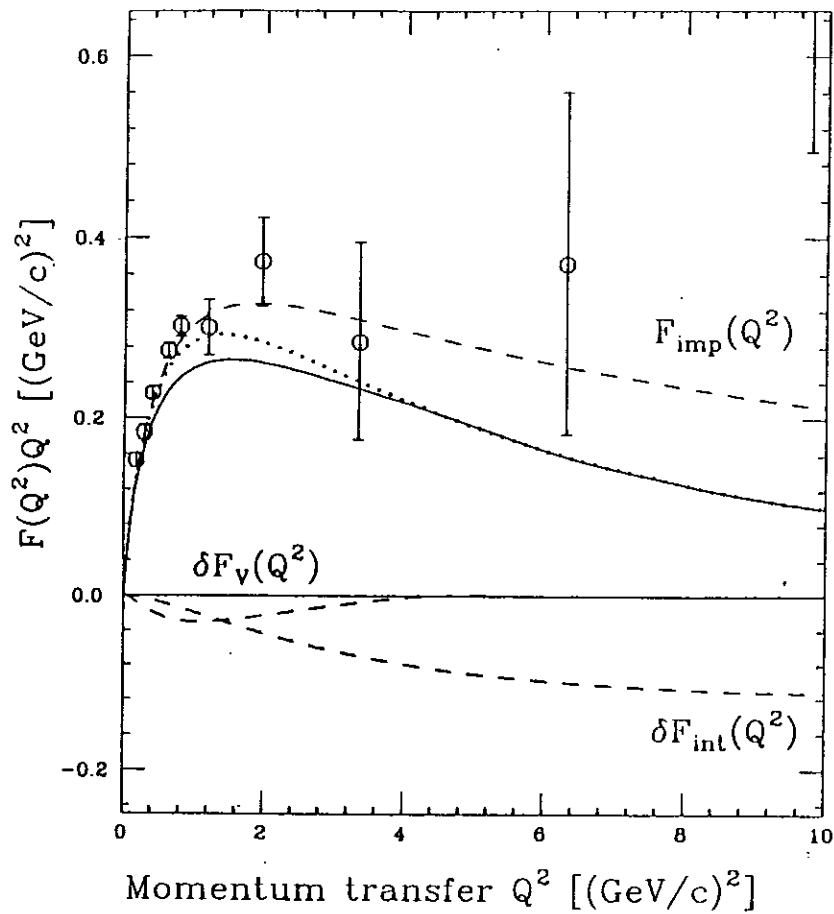


Fig. 23

The pion charge form factor multiplied by  $Q^2$ . Separate contributions from the impulse ( $F_{imp}(Q^2)$ ), interaction current ( $\delta F_{int}(Q^2)$ ) and vector channel ( $\delta F_V(Q^2)$ ) form factors are shown as dashed lines. The solid line is the total result, and the dotted line is the total amount without the vector channel contribution. The experimental data are from Ref. 45.

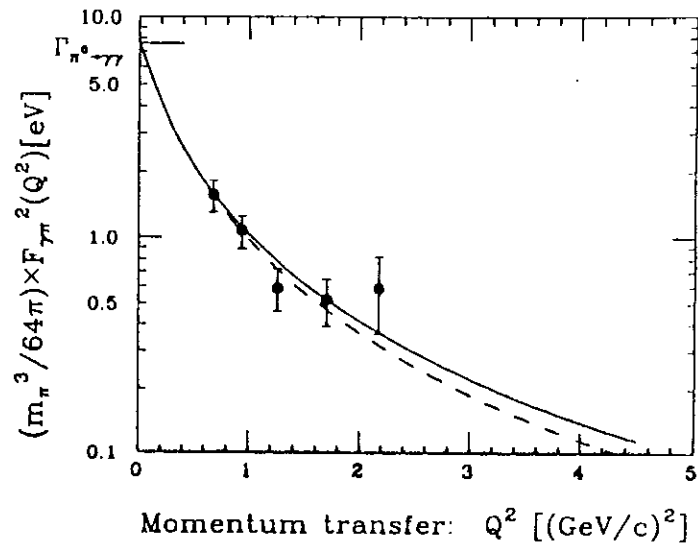


Fig. 24

The transition form factor of  $\gamma^* \pi^0 \rightarrow \gamma$  reaction, where the virtual photon carries space-like momentum,  $q^2 = -Q^2 < 0$ . The solid line is our prediction with the parameters,  $m_q = 248 MeV$  and  $\Lambda = 450 MeV$ . The dashed line is the prediction with the hadronic Vector Meson Dominance model. The experimental data are given by Ref.38.

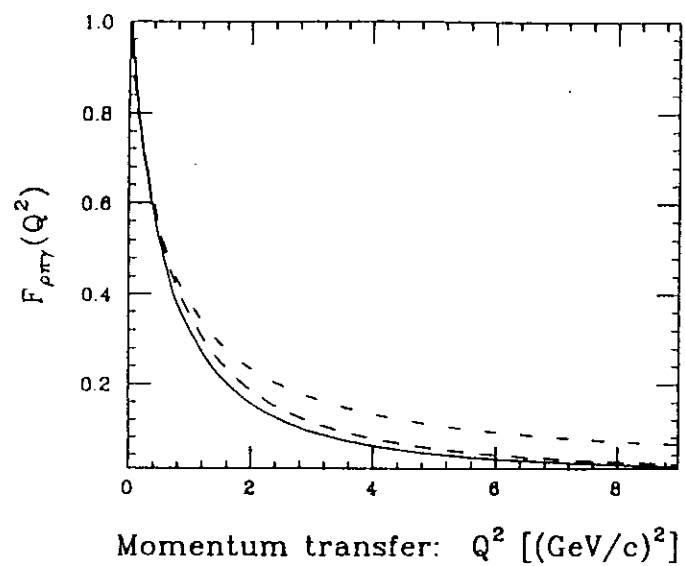


Fig. 25

The form factor for the  $\rho\pi\gamma$  coupling for space-like photons,  $q^2 = -Q^2 < 0$ . The solid (dotdash) line is our prediction with the parameters,  $m_\rho = 248 \text{ MeV}$  and  $\Lambda = 450(550) \text{ MeV}$ . The dashed line is the prediction with the hadronic Vector Meson Dominance model<sup>17</sup>.